



*School of Mechanical and Systems Engineering*

---

# **The Engineering Of Masks For Application In Continuous Positive Airway Pressure (CPAP) Therapy**

---

---

**Undertaken By:** Ciaran Luke Doyle (140253267)  
**Module:** MEC3098  
**Date:** 15/05/2017  
**Academic Supervisors:** Dr Javier Munguia

---

## Declaration

---

This Report is submitted as part of the requirements for the Degree of Mechanical Engineering at the University of Newcastle upon Tyne and has not been submitted for any other degree at this or any other University. It is solely the work of Ciaran Doyle (UG) except where acknowledged in the text or the Acknowledgements below. It describes work carried out at the University of Newcastle upon Tyne which is entirely recorded in a Project Logbook which has been made available for examination. I am aware of the penalties for plagiarism, fabrication and unacknowledged syndication and declare that this Report is free of these.

## Acknowledgements

---

The Author would like to acknowledge the support, guidance and supervision provided by Dr Javier Munguia. Additional acknowledgements are made to Dr Philip Hyde and PhD student Zhichao Mao, who is engaged with a similar related project, for allowing the Author of this report to attend their student/supervisor meetings, and for sharing ideas and resources.

## Abstract

---

Patient compliance with prescribed positive airway pressure therapy is cited to be as low as 50%, severely limiting the efficiency of said treatment. Given the wider CPAP system has continued to evolve, with recent progression in the use of humidifiers and sophisticated airflow control theoretically improving patient experience, this project set out to establish the engineering theory of mask design and how it may be limiting therapy success.

In order to do so it was first necessary to establish the principles of CPAP operation to better comprehend the role of the mask and the considerations influencing its design. This was achieved through analysis and evaluation of relevant literature, namely medical journals, identifying qualities key to a successful mask such as the prevention of CO<sub>2</sub> rebreathing and acceptance of the interface by the patient. Further exploration was carried out through the evaluation of commercial models, investigating factors such as design variety and material choice. Having identified amongst other areas that mask customisability offers a potential avenue for mask improvement, practical work was undertaken in the development of a CAD model. The purpose of this was to explore how top down assembly modelling can be used to adapt the geometry of a successful commercial model for customisation to digitised facial data. This work was supported by a brief demonstration of how finite element analysis can be used to inform the design process.

Following this, critical thought was applied to how these techniques are used in an industrial setting, with consideration being made for aspects such as the logistics and economics of customisation and the need to clinically evaluate and refine mask performance. Later research focused on emerging concepts being developed which may facilitate improved patient compliance. Having conducted a thorough research based investigation supplemented by practical work, this project culminated in the comprehensive review of CPAP mask engineering presented within this report.

---

## Contents

---

<b>1. Introduction</b>	
1.1. Project Aims & Objectives.....	1
1.2. Medical Theory.....	2
1.3. Positive Airway Pressure (PAP) Distinctions.....	3
1.4. The Modern CPAP System.....	4
<b>2. CPAP Mask Design Considerations</b>	
2.1. Design Elements.....	5
2.2. Regulations & Governing Bodies.....	6
<b>3. Commercial CPAP Mask Design</b>	
3.1. Over-engineering & Requisite For Design Variety.....	9
3.2. Mask Design Selection.....	10
3.3. Material Choice.....	11
3.3.1. Polycarbonate.....	11
3.3.2. Silicone.....	11
3.3.3. Polyethylene.....	11
<b>4. Specifics Of CPAP Mask Optimisation</b>	
4.1. CO <sub>2</sub> Rebreathing Reduction.....	11
4.2. Patient/System Interface Customisation.....	14
<b>5. CPAP Mask Design Methodology</b>	
5.1. Top Down Assembly Modelling.....	15
5.2. Design Schematics.....	17
5.3. Methods Of Facial Data Acquisition.....	18
<b>6. Design Development</b>	
6.1. Obtaining Facial Data.....	18
6.2. Custom CAD Model.....	19
6.3. Finite Element Analysis (FEA).....	21
<b>7. Discussion</b>	
7.1. Evaluation Of CPAP Mask Design Method.....	25
7.2. Further Use Of Computational Modelling.....	26
7.3. Assessing CPAP Mask Performance.....	27
<b>8. Developing CPAP Mask Concepts</b> .....	28
<b>9. Conclusion</b> .....	29
<b>10. Future Work</b> .....	30
<b>11. References</b> .....	30
<b>12. Appendices</b> .....	35

---

## Figures

---

Figure 1: Typical features found on commercial CPAP masks (ComfortFull 2 by Phillips Respironics).....	1
Figure 2: The splinting effect of positive airway pressure on the upper respiratory tract.....	2
Figure 3: The various physiological mechanisms by which CPAP therapy aids respiratory function.....	2
Figure 4: Contrasting flow profiles of CPAP and BiPAP airflow delivery.....	3
Figure 5: The Bloxsom Positive Pressure Oxygen Air Lock Device.....	4
Figure 6: Block system diagram of a typical CPAP system. Note the role of the mask as the system/patient interface.....	4
Figure 7: The upper respiratory tract through which air is delivered during CPAP.....	5
Figure 8: Severe septal erosion of a neonate receiving CPAP therapy.....	6
Figure 9: The scope of ISO 17510-1 and 17510-2.....	7
Figure 10: Fixed orifice diffuser schematic.....	11
Figure 11: Flow contraction through a fixed orifice.....	12
Figure 12: The effect of a non-breathing valve during CPAP system failure.....	13
Figure 13: Mass produced CPAP mask cushion with excess material intended to deform to fit the patients face.....	14
Figure 14: Patient wearing silastic prosthetic, with and without CPAP mask.....	14
Figure 15: The production of a customised CPAP mask cushion for a patient with craniofacial anomalies.....	15
Figure 16: An example of top down design modelling being used to identify key geometry, aiding the design process of a knee brace.....	16
Figure 17: Anatomical reference planes which can be used as datums in the engineering of CPAP masks.....	16
Figure 18: Top down component design approach used to decompose complex assemblies.....	17
Figure 19: The decomposed Eson 2 mask schematic. This diagram easily allows the identification of key geometry such as that between the joint socket and ball. KEY: red=root, yellow=sub assembly, blue=part:.....	17
Figure 20: The facial data before and after post processing.....	19
Figure 21: Annotated facial data with key geometry identified.....	19
Figure 22: Hose connector.....	20
Figure 23: Frame and joint socket sub assembly.....	20
Figure 24: Geometry on socket face used to orientate the mask cushion.....	20
Figure 25: Master assembly with the cushion/frame intermediary removed, with sketch lines to show flow alignment with nasal orifice.....	21
Figure 26: Splines were created from point geometry which were then patched and stitched together to create the functional surface of the bust for use in finite element analysis.....	22
Figure 27: Forces modelled in FEA analysis.....	22
Figure 28: Graph to show mesh independence reached when mesh reduced to 0.45mm....	23
Figure 29: FEA analysis using silicone rubber as the cushion material. Average element equivalent Von Mises stress was 0.004137 MPa. Note how the areas of high stress are more evenly distributed than when other materials are used.....	23
Figure 30: FEA analysis using natural rubber as the cushion material. Average element equivalent Von Mises stress was 0.004244475 MPa.....	24
Figure 31: FEA analysis using silicone elastomer as the cushion material. Average element equivalent Von Mises stress was 0.004147926 MPa.....	24
Figure 32: Customised headphone inserts by Earcandi.....	25

---

Figure 33: Facial scan data taken from a realistic infant doll for the intent of developing a neonatal CPAP mask .....	25
Figure 34: Spinal vertebrae made in MIMICS, displaying various mesh configurations .....	26
Figure 35: FEA can be used in a range of applications, such as creating temperature and velocity plots to identify probable areas of condensation formation .....	26
Figure 36: A lung simulator with various component labelled such as face mask (FM) and anatomical deadspace (AD) .....	27
Figure 37: Flow data of the Eson 2, with and without diffusor attached .....	28
Figure 38: Concept of a variable diffusor design .....	28
Figure 39: CPAP head helmet design .....	29

## Tables

Table 1: The six distinctive classes of CPAP masks .....	8
Table 2: OSA sufferer demographics .....	9
Table 3: Example table used to assess mask design appropriateness for a patient .....	10
Table 4: Typical CPAP mask bill of materials (FlexiFit 407 by Fischer & Paykel Healthcare) .....	10

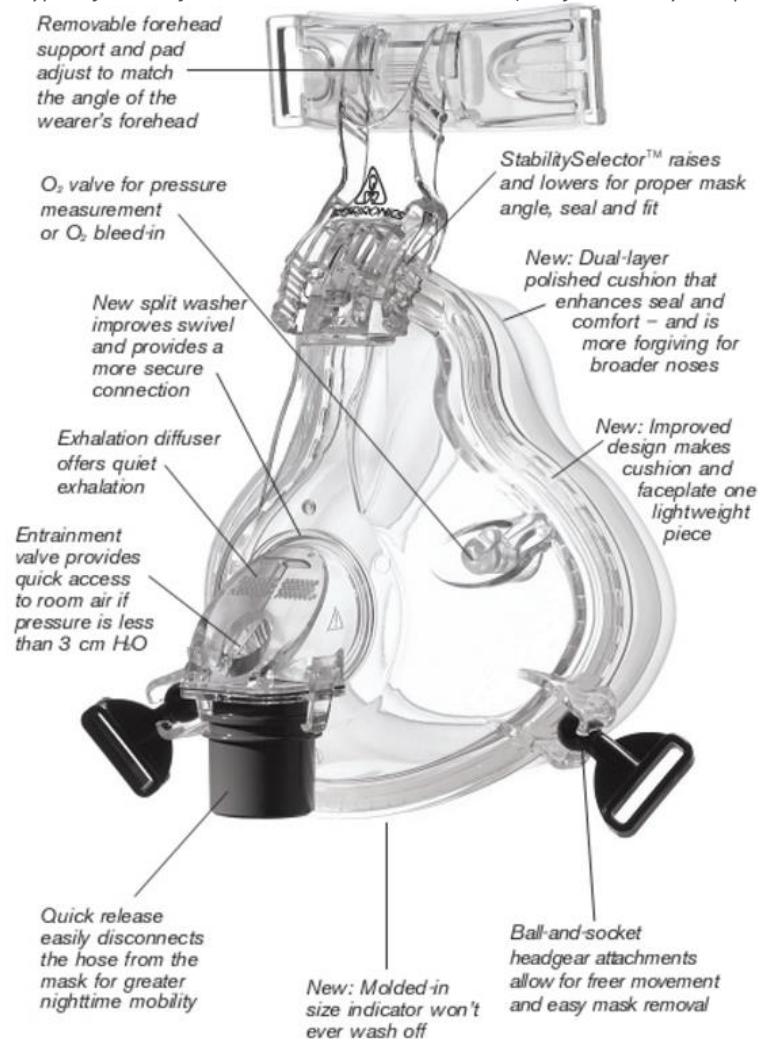
## Nomenclature

Symbol	Quantity
$\dot{m}_b$	Mass flow rate of air through orifice
$\dot{m}_t$	Mass flow rate of air through tube system
$\dot{m}_p$	Mass flow rate of air from patient
$P_m$	Pressure within mask
$m_m$	Total mass of air within mask
$\rho_a$	Mask air density
$A_b$	Orifice cross sectional area
$C_d$	Discharge coefficient
$Q_b$	Vent volume rate
$n$	Number of orifices venting air from mask
$A_{vc}$	Cross-sectional area of the vena contracta
$A_u$	Upstream cross-sectional area
$C_v$	Flow velocity coefficient
$C_c$	Area contraction coefficient
$C_{d\infty}$	Turbulent discharge coefficient
$\delta_1, \delta_2$	Laminar discharge coefficients
$a, b$	Shape coefficients

## 1. Introduction

Continuous positive airway pressure (CPAP) therapy refers to the medical practice of supplying a pressurised flow of air to keep the airways open in patients unable to do so autonomously. CPAP is used to treat a range of chronic medical conditions, it being the most common treatment method for obstructive sleep apnoea (OSA), and is widely used in the alleviation of complications arising from other obstructive airway diseases.<sup>[1]</sup> In addition, CPAP is playing a growing role in emergency care, having successfully being used in the treatment of acute diseases such as infant respiratory distress syndrome (IRDS), congestive cardiac failure and pulmonary oedema.<sup>[2]</sup> Mask design constitutes a fundamental part of successful CPAP therapy, competitive models exhibiting a number of features adapting the mask for its role in the wider CPAP system.

Figure 1: Typical features found on commercial CPAP masks (ComfortFull 2 by Phillips Respironics)



### 1.1. Project Aims & Objectives

This project has set out to achieve the following, the results of which are summarised in this report:

- To establish the use of CPAP therapy and the role of the mask within the wider CPAP system
- To determine parameters influencing mask design
- To evaluate the design and application of commercial CPAP masks
- To explore specifics of mask optimisation
- To review design methodology for use in CPAP mask development



In addition, practical investigation of the above was undertaken in the form of the CAD development of a typical CPAP mask model, for the purpose of deepening the Authors understanding of the engineering processes involved.

The main deliverable of this project is a comprehensive and systematic review of the engineering of CPAP masks, in the form of a report document.

## 1.2. Medical Theory

The efficacy of positive airway pressure therapy is due to a number of physiological mechanisms. The most prominent observations are the effects found on the upper airway, in particular the pharyngeal area, the constriction of which is symptomatic in a number of diseases. Untreated constriction reduces patient airflow and can result in apnoeas, temporary cessations in breathing, or hypopneas, periodic reductions in airflow resulting in a decrease in oxyhemoglobin saturation.<sup>[3]</sup> The pressure differential provided by therapy results in increased hoop stresses in the airways which, given the closed nature of the respiratory system, provide axial stresses that act to open the airway tract. This effect is mirrored on the lungs themselves, reducing the work required by respiratory muscles such as the diaphragm and intercostals.<sup>[4]</sup>

A second, more often overlooked effect of positive airway pressure therapy is the prevention of bronchiole and alveoli cavity collapse at the end of expiration, which under normal conditions follow a cycle of near complete inflation and deflation. In accordance with Young's-Laplace law, a fully collapsed volume requires significantly higher pressure to restart expansion, which in this context begins with each new patient inspiration.<sup>[5]</sup> If the term compliance is used to describe the relative ease of inflation, the alveoli can be described as operating at a higher compliance whilst partially inflated during the majority of the respiratory cycle, compared to their compliance when collapsed. PAP provides persistent alveoli dilation which prevents alveoli from collapsing to a lower compliance state, in turn reducing the work required to initiate re-inflation of the alveoli during inspiration.<sup>[6]</sup> In addition to providing a more expanded lung resting position, the constant expansion of the bronchioles and alveoli is found to allow more complete blood flow circulation, increasing perfusion of CO<sub>2</sub> and O<sub>2</sub>.<sup>[7]</sup>

Figure 2: The splinting effect of positive airway pressure on the upper respiratory tract

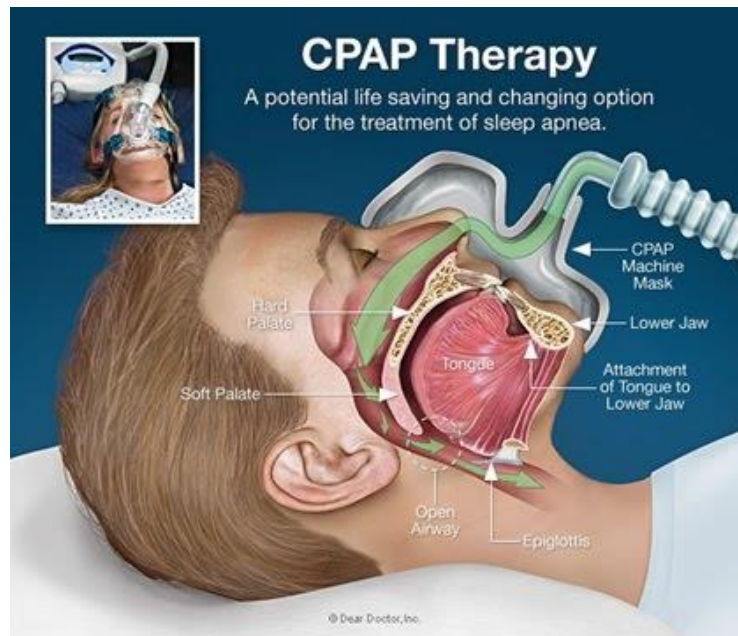
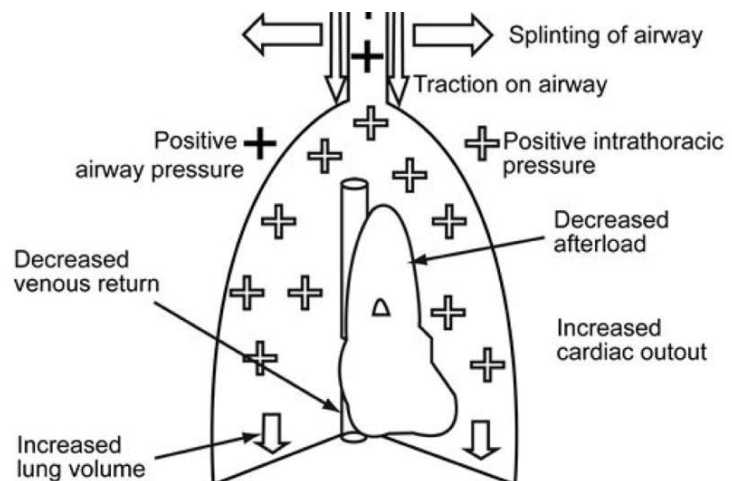


Figure 3: The various physiological mechanisms by which CPAP therapy aids respiratory function



### 1.3. Positive Airway Pressure (PAP) Distinctions

PAP is an umbrella term covering a number of airflow delivery methods. Fixed pressure therapy, where the airflow is delivered at a constant pressure, is referred to as continuous positive airway pressure (CPAP) treatment and is the most common method of PAP delivery.<sup>[8]</sup> The emergence of sophisticated micro controllers has allowed for the development of auto titrating (APAP) delivery systems where the airflow at the patient end is constantly monitored and adjusted to ensure it is of constant pressure. APAP should not be seen as discrete from CPAP, moreover it is a development intended to accommodate for pressure swings and loss throughout the system, the result being a truer CPAP airflow.<sup>[9]</sup>

Although CPAP is the most widely used method of airflow delivery, some patients such as preterm infants experience difficulty when exhaling against a fixed pressure. In such cases Bi-PAP delivery may be appropriate. During Bi-PAP supplied pressure is reduced during the expiratory phase. The purpose being to reduce

the resistance which must be overcome by the patient to expel waste respiratory gases. Theoretically this will decrease respiratory muscle recruitment, allowing patients to breathe with greater ease.<sup>[10]</sup> This technique was pioneered for use in patients where maintaining constant levels of intra-airway pressure poses the risk of barotrauma or ventilatory depression, such as in pre term infants whose lungs may have not fully developed.<sup>[11]</sup>

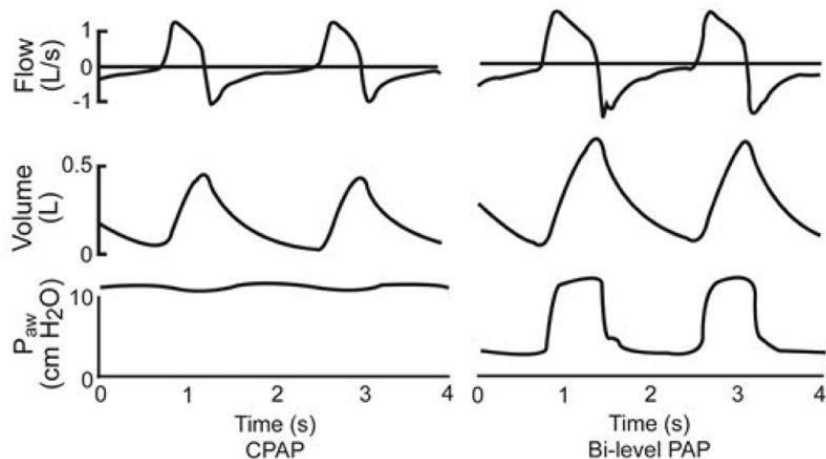


Figure 4: Contrasting flow profiles of CPAP and BiPAP airflow delivery

Bi-PAPs physiological advantages have however not manifested themselves in increased rates of patient compliance within the general population prescribed therapy, a Cochrane database review observing negligible difference between Bi-PAP and CPAP therapies from an adherence perspective.<sup>[12]</sup> Considering there is a scientifically verified improvement in PAP delivery which has not resulted in significant improvements in patient experience, this points to other areas of the PAP machine as limiting performance. This highlights the key role components other than the PAP machine itself have to play in the effectiveness of PAP therapy, notably those such as the mask which will be discussed in this report.

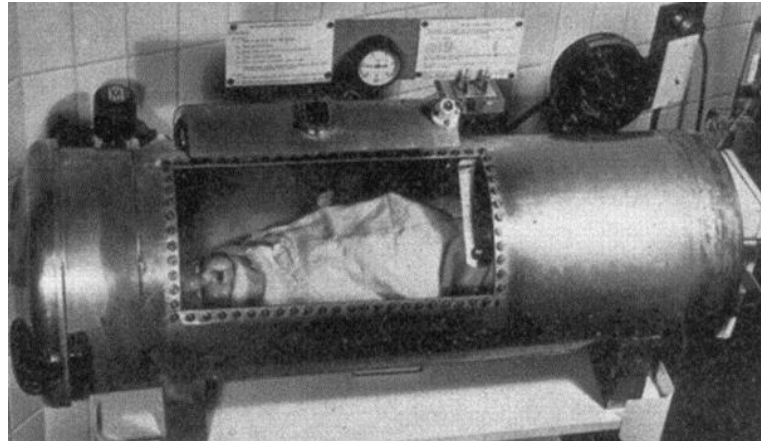
The design of masks for use in PAP therapy is largely independent of airflow delivery specifics, most commercially available masks being compatible with both CPAP and Bi-PAP machines. However the constant pressures involved in CPAP simplify analysis relevant to issues such as CO<sub>2</sub> rebreathing and, given its more general use, the scope of this project will focus principally on masks for use with CPAP therapy.

### 1.4. The Modern CPAP System

Whilst this project is concerned principally with mask design, an understanding of the wider CPAP system will help to comprehend the role of the mask and the part it plays within successful PAP therapy, informing mask functionality.



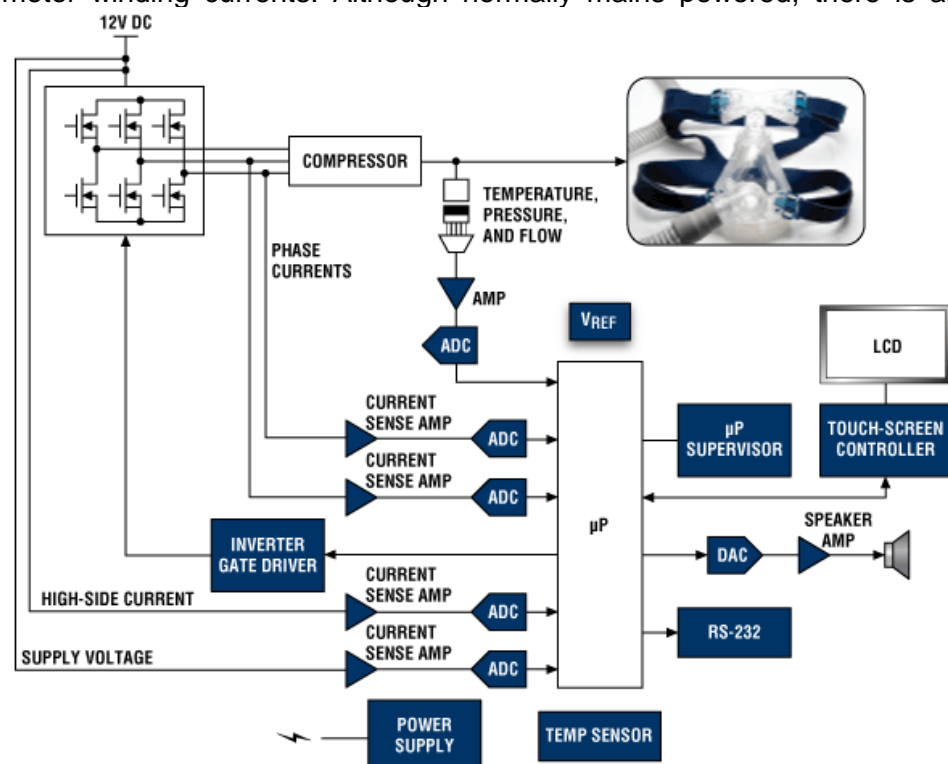
The first CPAP commercial model was made available in North America in 1980, prior to which CPAP therapy had largely been contained to hospital environments. Prior to the development of what would be recognisable as the masks of today, non-invasive ventilation therapy was delivered in a range of now antiquated methods, such as the iron lung or Bloxsum air lock, used in the treatment of neonates.<sup>[13]</sup>



Since the emergence of commercial models, the market has grown to be valued at an estimated \$4.59billion, and is currently expanding at an annual rate of 7.9%.<sup>[14]</sup> Companies such as Phillips Respironics, Fischer & Paykel Healthcare and Resmed have emerged and driven the design of CPAP systems forward as they compete for market share. The modern CPAP system is complex and can broadly be split into 3 distinct areas: 1) the CPAP machine itself, 2) the hose system used to deliver airflow, and 3) the mask/patient connection. The mask forms a seal to the patients face, allowing a continuous source of compressed air to pressurise and open the patients' airway. Mask air is monitored by input sensors that measure flow temperature, humidity and pressure, providing feedback to the machine microprocessor controller. The specific method of feedback varies between models, some using a pneumatograph to quantify flow characteristics whilst others detect variation in blower rotation speed. The microprocessor in turn controls the motor used to maintain desired airflow, which is done by varying fan velocity.<sup>[9]</sup>

The blower motor, which typically runs from a DC voltage of 12-24V, can operate in ranges from 1000 RPM up to 30-40 kRPM. However, more important than the extremes of speed achievable is the ability to rapidly adjust to match changes in the patient environment, requiring monitoring of the motor winding currents. Although normally mains powered, there is an

Figure 6: Block system diagram of a typical CPAP system. Note the role of the mask as the system/patient interface



increasing demand for battery powered models which are being developed in tandem with smaller CPAP machines to allow a greater level of portability. The ability to display information to medical operatives and to output audio alerts in the event of machine failure are also integral to a successful CPAP machine. The block diagram in Figure 6 shows how these functions are combined within a typical CPAP system, highlighting the role of the mask as the system patient interface.<sup>[15]</sup>

## 2. CPAP Mask Design Considerations

Taking into account the crucial role of the mask as the patient/system interface, there are many aspects to be evaluated when designing masks for use in CPAP therapy. As with all medical devices there are stringent guidelines in place to regulate product quality. These various design considerations and controls are discussed within this report section.

### 2.1. Design Elements

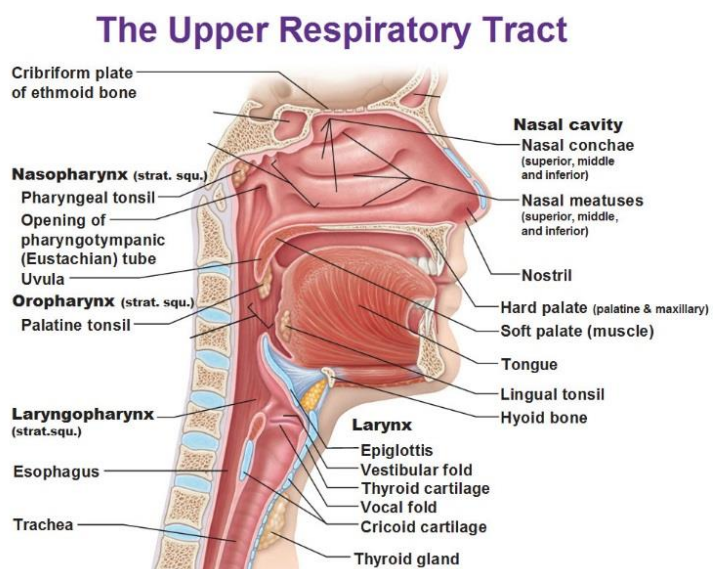
To illustrate the significant challenges which must be overcome, patient adherence and long term compliance with prescribed CPAP therapy is often found to be as low as 50%.<sup>[3]</sup> Moreover, in a study by Wedzicha, et al. it was determined that for all patients involved, 53% experienced disruption to treatment solely due to reported mask discomfort.<sup>[16]</sup>

Simplifying this issue by disregarding patient comfort, from a purely functional perspective a CPAP mask must be capable of maintaining a seal at operating pressures, otherwise treatment efficiency is significantly reduced. Operating pressures vary on a patient by patient basis and are dependent upon the force required to appropriately open the airways, determined by a clinician. Typical ranges are from 4-20 cm H<sub>2</sub>O or approximately 400-2000 Pa. Furthermore, in reality the mask must be capable of maintaining this seal during the patients' sleep, during which a high level of nocturnal activity increases the risk of the mask being dislodged.<sup>[10]</sup>

Figure 7: The upper respiratory tract through which air is delivered during CPAP

It is of note that where the higher range of airflow pressures are required, patients demonstrate a preference for oral as opposed to nasal delivery, reporting discomfort on the smaller incident area of the nares.<sup>[3]</sup> Despite this, a systematic review of CPAP efficacy observed that purely oral, purely nasal, or delivery via a combination of oro-nasal methods all resulted in improvements in patients diagnosed with OSA.<sup>[17]</sup>

The patient/system interaction cannot be seen as a one way exchange given gases are exhaled by the mask wearer, CO<sub>2</sub> constituting approximately 5% by volume of the exhalant profile.<sup>[18]</sup> This is clinically significant as CO<sub>2</sub> is an asphyxiant and at high concentrations can induce tachycardia and impaired consciousness, leading to convulsions and coma at concentrations >10%.<sup>[19]</sup> This is particularly relevant considering patients prescribed CPAP therapy already suffer from respiratory difficulties, Farre, et al. finding that CO<sub>2</sub> rebreathing could be so detrimental to therapy so as to render it ineffective.<sup>[20]</sup> Consequently it is of paramount importance that masks have a mechanism through which to dispel exhaled gases.



An often cited reason for noncompliance, especially associated with older CPAP machines, is airway dehydration due to the increased airflow patients' experience. This abnormal microclimate manifests itself in patients complaining of rhinitis, rhinorrhoea, nasal congestion and oral dryness.<sup>[3]</sup> Modern CPAP machines attempt to overcome this issue through the use of a humidifier to moisturise the delivered airflow.<sup>[21]</sup> However, air of increased humidity is associated with increased levels of condensation forming within the mask. This is detrimental to CPAP therapy, both from a patient comfort perspective and regarding actual CPAP performance, as condensation within the system reduces the lumen of the airflow delivery hose.<sup>[22]</sup> considering humidity is tailored to individual patient preference, mass produced masks must be capable of functioning in a range of potential humidities and be designed to reduce collection of condensation.

Considering the chronic nature of many *Figure 8: Severe septal erosion of a neonate receiving CPAP therapy*

of the diseases which PAP therapy is used to treat and the extended periods of contact associated with the nocturnal wearing of masks, local skin irritation frequently develops. This potentially leads to epidermal breakdown and even ulceration. In a study into domiciliary CPAP use, Wedzicha, et al. classified patient skin irritation into two categories, the terms major referring to broken skin or open



sores and minor being used to describe persistent areas of red or painful skin. Over a median treatment period of 16 months, of the patients involved in the study 17% reported major complications whilst 38% reported minor complaints, arising from an average daily mask use of 7 hours.<sup>[16]</sup> The occurrence of such complications inhibits long term patient compliance which is necessary for effective therapy, and as such proper mask design must attempt to address issues such as the magnitude and distribution of forces within contact areas.

Additional design parameters relating to the inherent complexity and sensitivity of the facial area with which the mask interacts must also be taken into account. For example, manufacturers must endeavour to use odourless materials for the mask interior and efforts must be made to both reduce physical mask size and the use of opaque materials, obtrusive masks being associated with patient complaints of claustrophobia.<sup>[3]</sup>

## 2.2. Regulations & Governing Bodies

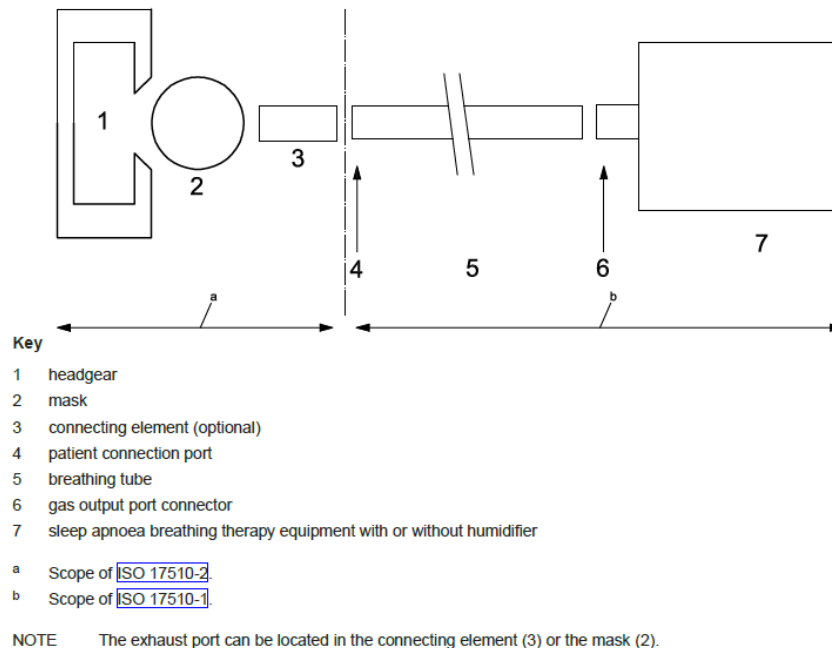
'BS EN ISO 17510: Sleep apnoea breathing therapy' details a number of standards pertaining to CPAP systems and is separated into two sections; BS EN ISO 17510-1 is relevant to sleep apnoea breathing therapy equipment whilst ISO 17510-2 covers masks and application accessories. These standards apply to equipment intended for use with adults and children, there scope not encompassing devices for use with neonates.<sup>[23]</sup>

In practical terms, part 2 expands to detail requirements for any necessary connecting element between the sleep apnoea breathing therapy equipment and the patient, such as headgear connecting ports and valves. Standards are outlined regarding the geometry of certain components, for example it is stated that 'mask connectors, if conical, shall be 15 mm or 22 mm size male connectors conforming to ISO 5356-1: Anaesthetic and respiratory equipment. Non-conical mask connectors shall not engage with conical connectors conforming to ISO 5356-1 or ISO 5356-2, unless they comply with the engagement, disengagement and leakage requirements of ISO 5356-1 or ISO 5356-2'. It is also specified that masks must be designed such that they can be easily cleaned and contamination risks are minimised.<sup>[23]</sup>

ISO 10993: Biological evaluation of medical devices also influences CPAP mask design, categorising various components according to their patient interaction and describing regulations accordingly. Nasal and oral accessories are evaluated as mucosal membrane contacts whilst other mask materials contacting the patients head are evaluated as skin contacting. Due to mask use exceeding a cumulative 30 day period all mask materials are treated as permanent duration contact components and are subject to stringent biocompatibility requirements.<sup>[24]</sup>

BS EN ISO 17510-2:2009  
ISO 17510-2:2007(E)

Figure 9: The scope of ISO 17510-1 and 17510-2



Within the UK the regulation of CPAP masks falls under the jurisdiction of the Medicines & Healthcare products Regulatory Agency, an executive agency of the Department Of Health.

### 3. Commercial CPAP Mask Design

As discussed, there are numerous parameters such as operating pressure and humidity, which are tailored to individual patients needs, and have an impact on optimal mask design. In the absence of mass customisation manufacturers must therefore create a variety of masks compatible with a range of operating conditions, examined within section 3 of this report.

#### 3.1. Over-engineering & Requisite For Design Variety







From a technical perspective CPAP masks are over-engineered to accommodate for the most extreme patient cases, for example ISO 17510 specifies that all masks must maintain an operating seal at pressures up to 20 cm H<sub>2</sub>O regardless of their intended patient application.<sup>[23]</sup> This may in part account for the high prevalence of skin irritation as masks are most likely not optimally designed to maintain a seal at the system pressure they are operating at, and so patients either under or over tighten the head straps used to fit the masks. This over-engineering is a significant factor in the design of fixed orifice diffusers discussed in report section 4.1 'CO<sub>2</sub> Rebreathing Reduction'.

Regarding the success of prescribed PAP therapy, patient compliance is the most direct influencing factor, and so every effort must be made to accommodate patient preference.<sup>[3]</sup> Despite different airway delivery routes having little impact on CPAP efficacy, compatibility with a specific patients preferred method of breathing constitutes a significant factor in patient



adherence.<sup>[17]</sup> This is reflected in the range of models offered by manufacturers, which can be split into 6 categories:

*Table 1: The six distinctive classes of CPAP masks*

<b>Model</b>	<b>Description</b>
<b>Nasal Cushion Masks</b> 	NC models sit around the nostrils and rest against the nasal bridge to form a contained area for delivery of airflow down the nasal airway. They are recommended for use with patients who dominantly nasal breathe and are limited in their application with oral breathers or those with deviated septums. <sup>[25]</sup>
<b>Nasal Pillow Masks</b> 	NP masks principal contact area is two small cushions designed to insert into the patient nares, minimalising facial contact. They are most suitable for users who would wear NC models but find them too obtrusive or the fit too uncomfortable. The extremely localised delivery of pressured air directly to the nostrils is associated with increased dryness and a 'jetting' sensation. <sup>[25]</sup>
<b>Full Face Masks</b> 	FF masks are the most commonly used in a hospital setting where reliable airflow delivery takes precedence over patient comfort. As in NC masks a cushion is used to create a contained environment but in these models it encompasses both the oral and nasal orifices. FF masks are suitable in a domiciliary environment for those who are unsecure which breathing mode they prefer or who are prone to sinus issues. <sup>[25]</sup>
<b>Total Face Masks</b> 	TF masks have the same airway function as FF models but the skin contact areas are shifted away from the nasal bridge and mouth areas, potentially improving comfort depending on patient facial structure. User vision is increase but there is significant dead space within the mask, the effects of which are discussed in report section 4.1 <sup>[25]</sup>
<b>Oral Masks</b> 	O masks sit between the gums and lips, providing CPAP to the oral airway and are appropriate in those intolerant of nasal breathing. Given the relative sensitivity and moisture of the oral contact area compared to the nasal orifice, O masks have been linked to higher rates of infection and complications. <sup>[25]</sup>
<b>Hybrid Masks</b> 	H masks integrate an O and NP masks to supply airflow to both airways whilst being less obtrusive than FF masks and with significantly reduced dead space. They are however more difficult to secure in space, making them unsuitable for patients with high nocturnal activity levels, and suffer from the same jetting as NP models. <sup>[25]</sup>



### 3.2. Mask Design Selection

To illustrate the impact of patient context on appropriate mask design two hypothetical juxtaposed scenarios will be discussed, investigating the selection of CPAP masks for the treatment of a typical OSA sufferer and an infant with IRDS.

Given the prevalence of OSA, it being theorised to affect up to 5% of adults in western developed countries, significant research has been conducted into patient indicators and demographics. <sup>[26]</sup> This research concludes that overweight men, aged 55-60, with a neck thickness greater than 16 inches are most at risk. <sup>[27]</sup> For the purposes of this comparison the hypothetical OSA sufferer will be assumed to match this modal profile.

Table 2: OSA sufferer demographics

Country and reference	Population subjects	Age (years)	Criteria	Prevalence (%)
USA (225)	352 men 250 women	30–60 30–60	Hypersomnia and RDI>5	4.0 (M) 2.0 (F)
Spain (226)	2148 1050 men 1098 women	30–70	AHI >5 plus symptoms	6.5 (M) 3 (F)
USA (227)	4364 men Subsample: 741	20–100	AHI>10 plus daytime symptoms	3.3 45–64 years: 4.7
United Kingdom (228)	893 men	35–65	ODI <sub>4</sub> >20, symptomatic ODI <sub>4</sub> >10 ODI <sub>4</sub> >5	0.3 1.0 4.6
Australia (229)	294 men	40–65	RDI>10 Subjective EDS and RDI>5	10.0 3.0

RDI, respiratory disturbance index; AHI, apnea/hypopnea index; ODI<sub>4</sub>, oxygen desaturation > 4%; EDS, excessive daytime sleepiness; M, males; F, females.

Upon inspection of collated data a correlation is found between patient weight and required airflow pressure to open constricted airways, and so it will be assumed that the OSA sufferer in this scenario requires a high pressure in the range 15-20 cm H<sub>2</sub>O.<sup>[3]</sup> For the purposes of this comparison it will be assumed that the individual does not find nasal mask use appropriate at this pressure. In comparison, IRDS is most frequent in neonates less than 28 days who typically require treatment pressures in the range 2-5 cm H<sub>2</sub>O. <sup>[28]</sup>

It is evident that the same style mask will not be appropriate in both outlined patient cases but the correct mask choice is not clear. To aid selection it is recommended to assess the range of mask models discussed previously according to a number of simplified criteria, a potential example of which is outlined in Table 3.

Table 3: Example table used to assess mask design appropriateness for a patient

Criteria	Mask Model					
	NC	NP	FF	TF	O	H
Airflow Delivery Route	Nasal	Nasal	Oronasal	Oronasal	Oral	Oronasal
Skin Contact Area (less contact area is desirable)	Medium	Small	Large	Large	Small	Small
Fit Security (higher fit security is desirable)	High	Low	High	High	Low	Low
Vision Obstruction (less obstruction is desirable)	Medium	Low	High	Low	Low	Low
Volumetric Dead Space* (less volumetric dead space is desirable)	Medium	Small	Large	Large	Small	Small

\*Volumetric dead space is related to increased CO<sub>2</sub> rebreathing and is discussed in report section 4.1 'CO<sub>2</sub> Rebreathing Reduction'

Although these assessments are qualitative and can be regarded as oversimplifications, they aid in mask allocation and can be increased in complexity as appropriate. For the neonate suffering from IRDS it is paramount that skin contact be minimised, as the Young's modulus of neonate skin is relatively low and prone to damage.<sup>[29]</sup> Table 3 indicates that the nasal pillow and oral masks have the lowest skin contact areas with little other distinction between the two mask designs other than airway delivery route. Considering the fact a purely oral delivery is associated with an increased rate of infection, the use of an NP mask would be recommended in this scenario. This conclusion is supported by the use of nasal cannulae to treat infants on hospital wards.<sup>[30]</sup> By contrast, the OSA sufferer in this case study requires a non-nasal mask, limiting choice to FF, TF, O or H models. The choice could then be made on the patients preference for either fit security, favouring FF or TF masks, or reduced skin contact, favouring O or H varieties.

### 3.3. Material Choice

Complying with ISO 10933, which places stringent constraints on materials available for use in CPAP masks, there are trends observed in the material choice exhibited by the leading mask manufacturers.<sup>[24]</sup> Material listings for the popular FlexiFit 407 model, whose material choice is typical of commercial CPAP masks, are shown in Table 4, with a wider sampling contained in Report Appendices: Item 1.

Table 4: Typical CPAP mask bill of materials (FlexiFit 407 by Fischer & Paykel Healthcare)

FlexiFit™ 407

Component	Material
Mask Base	Polycarbonate (PC)
Elbow	Polycarbonate (PC)
Swivel	Polycarbonate (PC)
Silicone Seal	Silicone (LSR)
Forehead Cushion	Silicone (LSR)
Foam Cushion	Polyurethane foam
Glider™ Strap	Nylon (PA)
Stretchgear™ Headgear	Breathe-o-prene™ (Lycra™ / Polyurethane foam laminate)
Pressure Ports Connector (Euro Only)	Polycarbonate (PC) / Santoprene™ (TPE)

### 3.3.1. Polycarbonate

Polycarbonates, example properties of which are listed in Appendices: Item 2, have a relatively high Young's modulus and fracture toughness making them strong, tough materials with a high impact resistance. They satisfy ISO 10993 and are ratified for use in medical applications. Regarding their use in CPAP masks as the frame and bracket material of choice, they are light and can be made transparent, reducing mask obtrusiveness. They are classed as 4-5 according to EduPack mouldability processing ratings, indicating they can be easily moulded into the complex shapes found in mask geometry. <sup>[24][31]</sup>

### 3.3.2. Silicone

Silicones, also called polysiloxanes, have a low Young's modulus, high biocompatibility and high resistance to microbe growth, making them a frequently chosen material for mask cushion components. <sup>[32]</sup> A notable property of silicones, which is beneficial in the context of CPAP masks, is their high gas permeability; at room temperatures the permeability of silicone rubber for oxygen is 400x that of butyl rubber. This means where silicones contact the skin there will still be relatively high levels of aeration, which is found to promote dermal health. Additional silicone properties are listed in Appendices: Item 3. <sup>[33]</sup>

### 3.3.3. (Poly)urethane

Polyurethanes are the strongest elastomers, with yield and tensile strengths up to 51 MPa. Their high biocompatibility combined with their ease of foamability makes them an easy to form material for use in CPAP mask headgear. Polyurethane foam, as frequently listed in manufacturers' bill of materials, is cheap to manufacture in large quantities through combination and setting with polyurethanes, polyols, di-isocyanates and blowing agents. Additional silicone properties are listed in Appendices: Item 4. <sup>[34]</sup>

## 4. Specifics Of CPAP Mask Optimisation

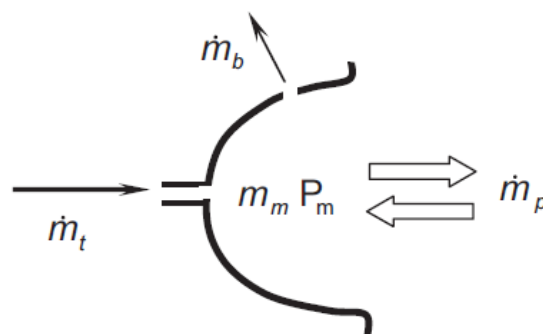
As determined in report section 2.1 'Design Elements' there are a number of critical mask design aspects which must be taken into account to facilitate successful CPAP therapy. The mask used must provide efficient airflow delivery whilst minimising risk to patients, and must do so in a way acceptable to patients to encourage long term compliance. Two specific ways in which CPAP mask are engineered to achieve these aims are discussed here.

### 4.1. CO<sub>2</sub> Rebreathing Reduction

As highlighted in report section 3.1 'Over-engineering & Requisite For Design Variety', due to CPAP systems single circuit design masks must have a mechanism by which to expel waste exhalant gases in order to prevent hazardous rebreathing. <sup>[35]</sup>

As well as being central to the therapy itself, most systems utilise the positive airway pressure supplied by the PAP system to provide the mechanism through which waste gases are expelled. <sup>[36]</sup> Typically this is done with the use of fixed orifice diffusers, which provide a route of low resistance for exhaled gases to be expelled from the system, relative to the high pressure airflow arriving from the CPAP machine <sup>[37]</sup>. Figure 10 shows a simplified schematic of a fixed orifice diffuser in operation, where  $\dot{m}_b$ ,  $\dot{m}_t$  and  $\dot{m}_p$  refer to the mass flow rate of air through the orifice, tube system and

Figure 10: Fixed orifice diffuser schematic



patient respectively,  $P_m$  describes the pressure within the mask and  $m_m$  is the total mass of air within the mask.<sup>[38]</sup>

The use of fixed orifice diffusers has been studied extensively and they are found to be a competent mechanism to reduce exhalant rebreathing. To demonstrate the effectiveness of the fixed orifice diffuser mechanism, Samolski, et al. conducted a study wherein a Bi-PAP system was used to deliver an inspiratory pressure of 14 cm H<sub>2</sub>O, whilst expiratory pressure was varied between 4, 6, 8 and 10 cm H<sub>2</sub>O. CO<sub>2</sub> levels within the masks tested were monitored during patient use, the authors finding that all the nasal masks tested displayed negligible CO<sub>2</sub> build up. Furthermore, an expiratory pressure of 4 cm H<sub>2</sub>O successfully prevented rebreathing in all conditions tested.<sup>[35]</sup>

The diameters of the orifices used in a specific mask are determined by the bias flow rate necessary to remove CO<sub>2</sub> from the CPAP system, calculation of the pressure differential between the mask environment and the ambient atmosphere being used to inform mask design.<sup>[37]</sup> Equation (1) shows the calculation of the pressure differential between the mask and the ambient where:  $\rho_a$  is mask air density,  $A_b$  is area of the diffuser orifice,  $C_d$  is the discharge coefficient and  $Q_b$  is the vent volume rate.  $A_b$  and  $\rho_a$  can be assumed to be constant whilst  $Q_b$  and  $C_d$  are found through further analysis.<sup>[38]</sup>

$$P_m - P_a = \frac{\rho_a}{2C_d^2 A_b^2} Q_b^2 \quad (1)$$

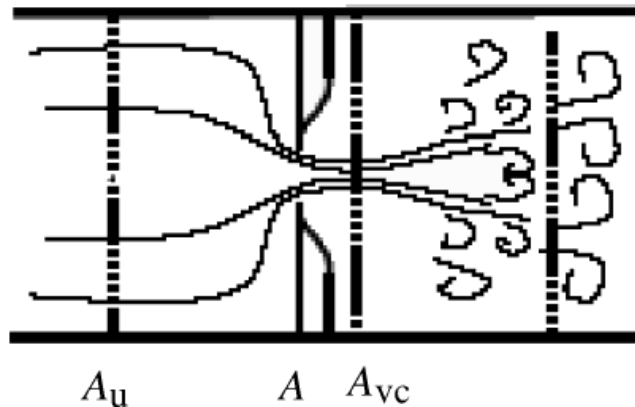
Vent volume flow rate is in turn governed by equation (2) where:  $n$  is the number of holes venting air from the mask.<sup>[38]</sup>

$$Q_b = \frac{\dot{m}_b}{\rho_a n} \quad (2)$$

Figure 11: Flow contraction through a fixed orifice

Defining Figure 11, where  $A_{vc}$  is the cross-sectional area of the vena contracta,  $A_u$  is the upstream cross-sectional area and  $A$  is the orifice cross-sectional area, it is possible to calculate the discharge coefficient. The formula for a single orifice is shown in equation (3) where:  $C_v$  is the flow velocity coefficient and  $C_c$  is area contraction coefficient.<sup>[37]</sup>

$$Cd = \frac{C_v C_c}{\sqrt{1 - C_c^2 (A_{vc}/A_u)^2}} \quad (3)$$



The following model shown in equation (4) can be used to approximate diffusers constituting numerous vents of differing geometries where:  $c_{d\infty}$  is the turbulent discharge coefficient for a chosen orifice,  $\delta_1$  and  $\delta_2$  refer to laminar discharge coefficient and  $a$  and  $b$  are shape coefficients.<sup>[39]</sup>

$$Cd = Cd_{\infty} \left( 1 + ae \frac{\delta 1}{Cd_{\infty} \sqrt{Re}} + be \frac{\delta 2}{Cd_{\infty} \sqrt{Re}} \right) \quad (4)$$

Regarding the application of these calculations it is demonstrated that the ability of a fixed rate diffuser to expel gases from a CPAP system operating at an exact pressure is dependent on the geometry and repeating units of the chosen diffuser, in addition to non-controllable variables such as atmospheric pressure. Experiments have shown that a bias flow rate >15 L/min reduces inspiratory fraction of CO<sub>2</sub> to 0.5%, a level deemed medically insignificant, with further increase in bias flow rate yielding no advantage. Moreover, a higher bias flow is associated with increased noise and pressure swings, both of which negatively affect patient compliance.<sup>[37]</sup> Considering all CPAP masks are required by ISO 17510 to adequately remove CO<sub>2</sub> at operating pressures as low as 4 cm H<sub>2</sub>O, it can be inferred that the bias flow rate of masks under realistic operating conditions results in unnecessary noise and pressure swings. This is unavoidable unless masks are classified and retailed according to their intended pressure use, which would require legislative change.

In addition to the bias flow rate, Schettino, et al. demonstrated that dead space within masks is associated with increased CO<sub>2</sub> rebreathing, and so successful mask design must attempt to reduce stagnant air volume. This was demonstrated by locating the exhalation port within the CPAP hose instead of within the mask itself, which was found to lead to greater levels of CO<sub>2</sub> build-up within the mask. Schettino, et al. postulated this was due to the larger dead space between the patient and exhalation port.<sup>[40]</sup> Reciprocating this conclusion, it has been found in other studies that exhalation ports placed directly over the nasal bridge offer improved flow characteristics to those placed elsewhere, leading to a reduction in rebreathing.<sup>[41]</sup>

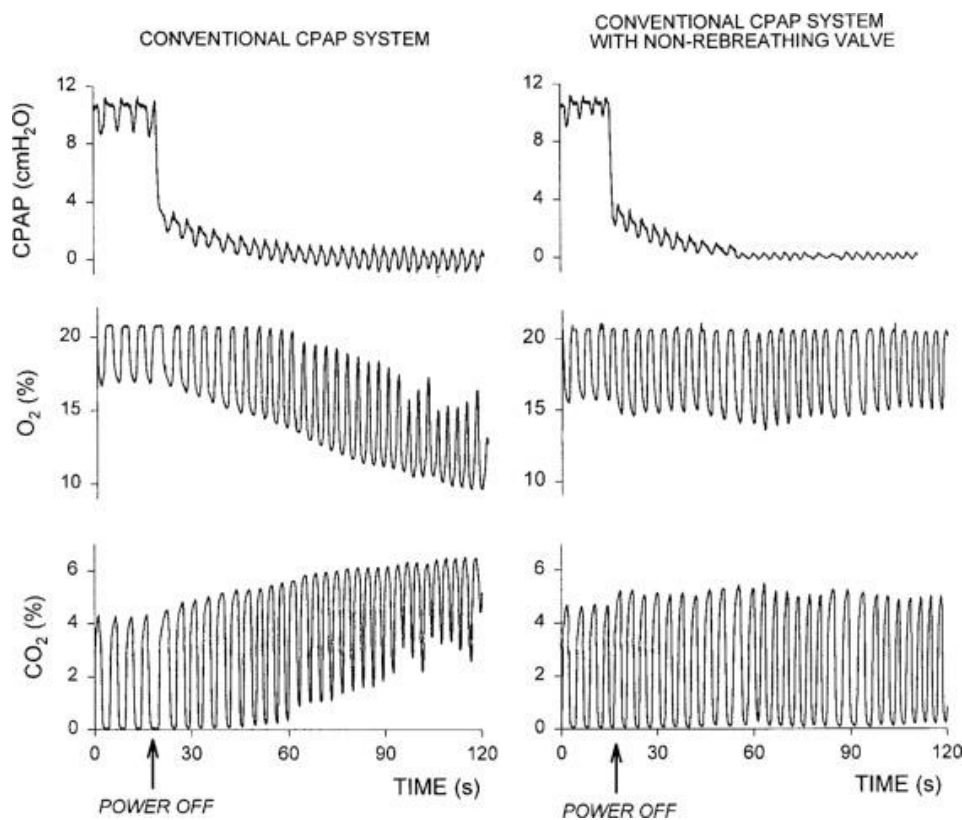


Figure 12: The effect of a non-breathing valve during CPAP system failure

Despite their effectiveness under ordinary operating conditions, the dependence of orifice diffuser functionality on a continuous supply of pressurised air forms a vulnerability which must be accounted for in mask design. Should the supply of pressurised air stop and the flow



resistance of the hose system to exhaled gases decrease, it has been found that the exhalation port would now offer the greater flow resistance. This would result in CO<sub>2</sub> being contained within the system and subsequent rebreathing would occur. This risk can be mitigated by the inclusion of a non-rebreathing valve into the mask, the effects of which are shown in Figure 12. Such a valve is closed under ordinary operating pressures but is designed to open should the air supply stop and internal pressures fall to equal atmospheric pressure.<sup>[36]</sup>

#### 4.2. Patient/System Interface Customisation

Patient compliance is critical to the success of all PAP therapy, a crucial aspect of which is acceptance of the mask patient interface.<sup>[16]</sup> Patients often exhibit a lack of satisfaction with mask fit, complications arising due to the relative complexity of the facial region and the fact commercial masks are only offered in a range of fixed sizes.<sup>[42]</sup> Manufacturers attempt to overcome this issue through the use of soft, padded materials around contact areas, and through the inclusion of excess cushion material intended to deform around a patients facial structure.

Although these features are beneficial, the performance of mass produced masks is ultimately limited by their lack of adaptability to a specific patient. As mentioned in report section 2.1 'Design Elements', Wedzicha, et al. found that 53% of patients curtail treatment solely due to mask discomfort, 24% do not adhere to therapy on at least one day per week, and 17% develop cutaneous complications. Lack of patient satisfaction with the mask patient interface is reflected in the fact that 36% of patients prescribed domiciliary CPAP therapy modify their masks in some way, the most often cited improvisations being the addition of cloth padding or foam wedges. Such modifications decrease seal quality, negatively impacting therapy effectiveness.<sup>[16]</sup>

In the same study it was found that the use of clinically moulded silastic prostheses, which over a four week period resolved all cases of ulceration, was beneficial to improving patient satisfaction whilst maintaining an effective seal. These moulds were formed from a compound applied directly to the patients' skin into which was pressed the CPAP mask, the resultant moulds subsequently being customised on each side to the patients face and mask respectively. The authors report the process took approximately 30 minutes and was simple to conduct.<sup>[16]</sup>

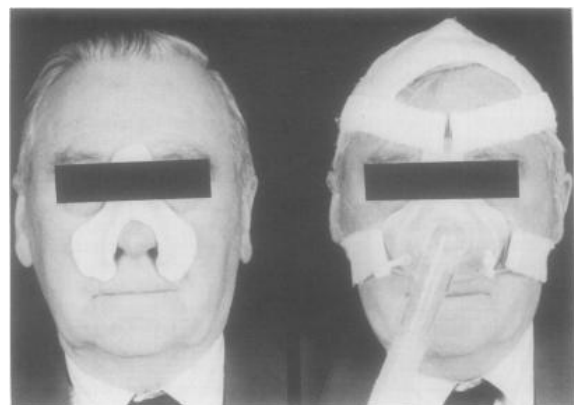
The fact that an interface moulded to match patients facial geometry will require less force to create a complete seal compared to standard issue masks, which require excessive force to deform the mask cushion to the patients facial structure, may be a factor contributing to their improved performance.<sup>[42]</sup>

Of particular relevance to the design of CPAP mask cushions is the fact OSA has an increased prevalence in individuals with craniofacial anomalies. This substantial demographic of users

Figure 13: Mass produced CPAP mask cushion with excess material intended to deform to fit the patients face

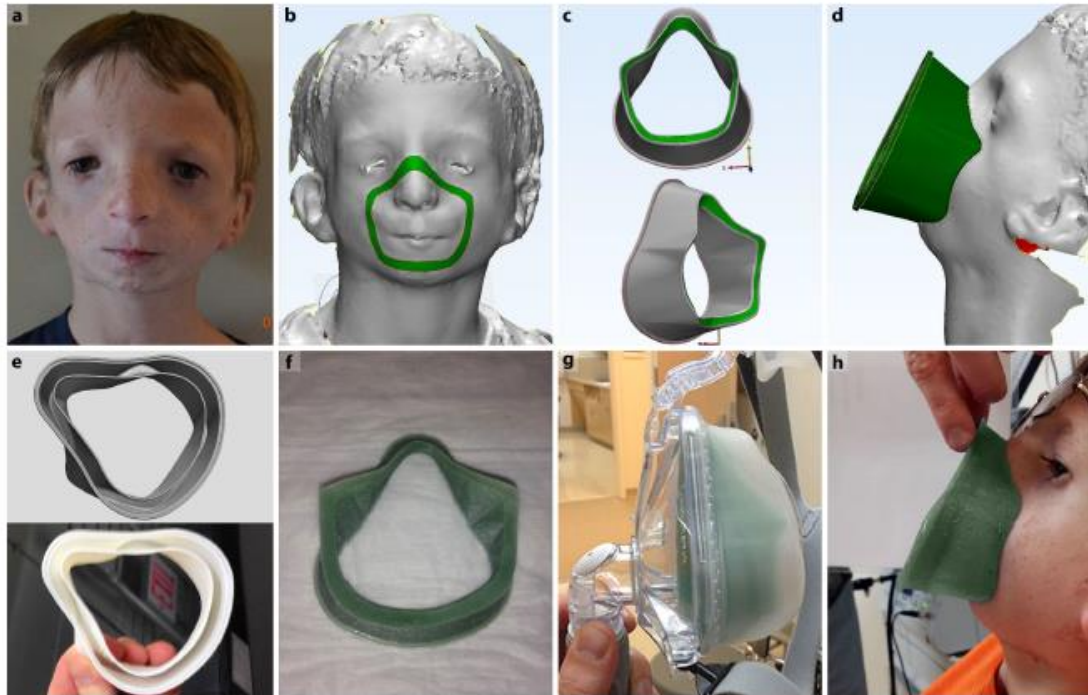


Figure 14: Patient wearing silastic prosthetic, with and without CPAP mask



experience increased complications with standard masks, notably in patients with abnormal midface and mandible development. An example study into the mask use of children suffering from Treacher-Collins syndrome found that customising the mask cushion decreased median leak from 25.2 L/min to 6.6 L/min, improved compliance over a one month period by 9%, and reduced patient apnoea/hypopnoea index by 24%.<sup>[43]</sup>

*Figure 15: The production of a customised CPAP mask cushion for a patient with craniofacial anomalies*



Customised components can be produced through a range of methods from rapid tooling and mould injection to 3D printing, these technologies having already been demonstrated to be economically viable in the in the production of customised orthodontics and in the treatment of burn victims requiring customised pressure masks.<sup>[43][44]</sup> Given their proven effectiveness, the appropriateness of custom produced components should be evaluated on a patient by patient cost to benefit basis. For example, complex components should be prioritised for users whose conditions are chronic as opposed to acute, where mask use is expected to terminate after a period. In acute cases the use of simple moulding techniques as demonstrated in the Wedzicha study would be recommended.

## 5. CPAP Mask Design Methodology

### 5.1 Top Down Assembly Modelling

The intricacy of the human body presents unique challenges in the engineering of devices which interface with anatomy, as products must take into account characteristics unique to the individual.<sup>[45]</sup> Variables such as the Young's modulus and thickness of an individual's skin are found to differ to a considerable extent, correlating with factors such as age and sex, whilst physical geometry deviates significantly from patient to patient.<sup>[29]</sup> Considering these challenges, design which makes use of a purely bottom up modelling approach has limited application, especially when applied to customisable biomechanical designs.

The term bottom up in this context describes the practice of modelling individual components to completion prior to the establishment of inter part relationships and constraints. This is contrasted with a top down approach to assembly modelling where a product overview is first ascertained and used to guide the development of components, iteratively refining them in a recursive process until complete. Top down design centres on the principle of utilising an assembly file to provide a global reference frame, making use of interdependencies between the base and its subsidiaries. In this way complex design tasks can be subdivided into smaller works, executable in tandem once inter component relationships are established.<sup>[45][46]</sup>

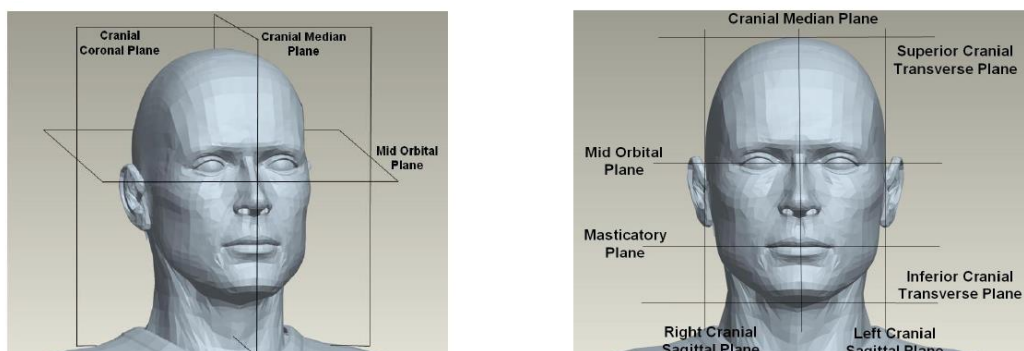
Figure 16: An example of top down design modelling being used to identify key geometry, aiding the design process of a knee brace



The parallelisability enabled by top down modelling makes design cooperation possible, as engineers can work independently on different components in the same assembly once its defining characteristics have been identified.<sup>[46]</sup> This holds particular relevance to the design of CPAP masks, where the ability to adapt components such as the mask cushion to a specific patient is desired. An example application could be the use of a small number of clinics to attain patient facial data which is uploaded to a master assembly, whilst engineers elsewhere who have a library of standard masks components complete the bulk of design work. Such an approach, combining certain aspects of top down and bottom up design, may work to offset the time delays and increased expense which traditionally limit customisation.

Chen, et al. establish a framework which can be used to apply a top down modelling approach to an engineering problem. In this methodology, contained in Appendices: Item 5, a product root is divided into various parts and subassemblies to which a top down component design approach is in turn applied. This process is repeated until the root product has been completely decomposed into its constituent parts. The top down component design schematic contained within the appendices highlights the iterative and systematic nature of this engineering approach, allowing large and complex design tasks to be tackled. For the design of anatomical garments, such as CPAP masks, Jensen, et al. propose the use of top down assembly modelling using digitised scan data as the assembly base. Medical and anatomical reference points could then be used as datums for reference geometry and mating conditions.<sup>[45]</sup>

Figure 17: Anatomical reference planes which can be used as datums in the engineering of CPAP masks



## 5.2. Design Schematics

As an example demonstration of how these techniques can be applied to CPAP mask design, root product decomposition was applied to the Eson 2 Nasal Mask, a commercial model by Fischer & Paykel healthcare. The top down component design approach outlined by Chen, et al. was used to decompose the Eson 2 into its base components.

*This schematic can in turn be used to identify key geometry and functional relationships between parts, which can be used to inform the design process. The decomposed Eson 2 mask schematic. This diagram easily allows the*

Figure 18: Top down component design approach used to decompose complex assemblies

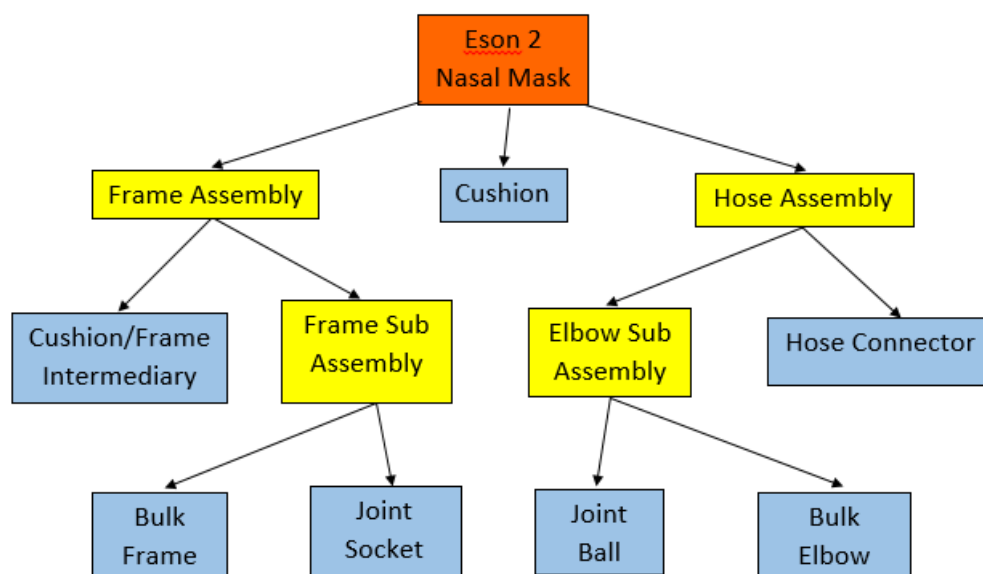
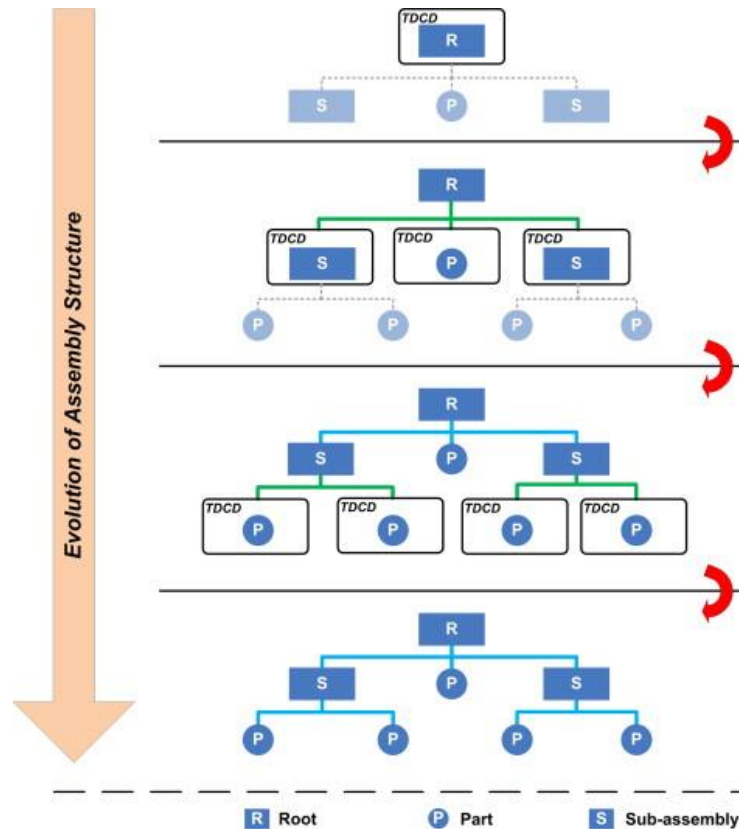


Figure 19: The decomposed Eson 2 mask schematic. This diagram easily allows the identification of key geometry such as that between the joint socket and ball. KEY: red=root, yellow=sub assembly, blue=part:



### 5.3. Methods Of Facial Data Acquisition

For the design of CPAP masks, especially masks containing customised components, the acquisition of facial data is fundamental to creating functioning products. For this purpose both contact and non-contact techniques can be used.

In the work of Cheng, et al., a dental impression material was adopted for use in taking an initial impression of the patients face for the manufacture of a customised CPAP mask. This was in turn converted to a hard plaster model which was scanned using a coordinate measuring machine to generate digitised facial data.<sup>[42]</sup> A similar approach to attaining facial data is also traditionally used in the manufacture of facial masks for pressure therapy of burn scars, where a plaster mould is produced from an alginate impression.<sup>[44]</sup>

Attaining data through contact methods, as opposed to using non-contact techniques such as laser scanning, has a number of limitations. Wei, et al. note that the taking of physical impressions presents difficulties, especially when applied to children, as some patients do not tolerate the impression taking process where no movement is permitted whilst the impression sets. An additional drawback of contact methods is the fact that with each additional process involved, namely the conversion of the initial impression to a plaster mould, accuracy is lost. To overcome these limitations Wei, et al. attempted to acquire burn victim facial data directly through the use of a Creaform Go Scan 50TM scanner set to a 1mm resolution. They found this method successfully allowed them attain facial data from otherwise uncooperative patients. Furthermore, they noted that the digital file format allowed editing of the geometry to create areas of higher and lower pressure when worn by the patients, a process which would have been complex to replicate with physical moulds.<sup>[44]</sup>

Following the success of the method explored by Wei, et al., it is a reasonable assumption that such an approach could be adapted for use in attaining CPAP patient facial data.

## 6. Design Development

---

Over the course of this project a CAD model has been developed to illustrate the design principles outlined in report section 5 'CPAP Mask Design Methodology' and how they can be applied to the development process of a typical CPAP mask. Basis of this model on the Eson 2 Nasal Mask by Fischer & Paykel Healthcare has additionally allowed investigation into how a commercially successful CPAP mask addresses the engineering considerations discussed throughout this report.

### 6.1. Obtaining facial data

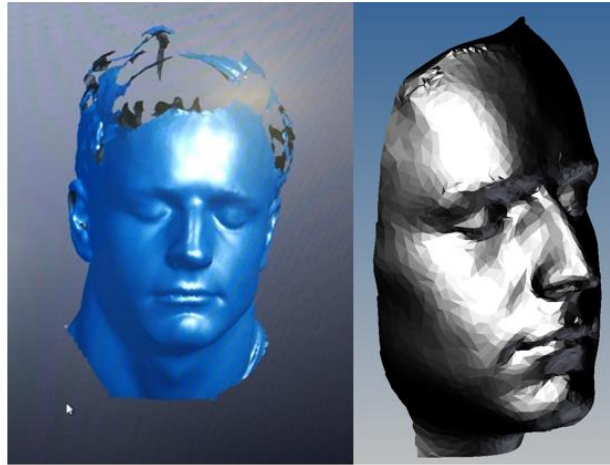
Providing the discussed advantages of personalised CPAP masks and the increasing prevalence of technology enabling such customisation, it was decided that the CAD demonstration in this section would contain a customised mask/patient interface. Limited available facial models of appropriate quality were found online and so obtainment of primary facial data was necessary.<sup>[47]</sup> Following ethical review in line with the guidelines established by Newcastle University the use of real patients was deemed beyond the scope of what this project aimed to achieve. However, the use of a peer volunteer was approved and a consenting individual was used for the purposes of this demonstration.<sup>[48]</sup>

Use of laser scanning technology was made to digitise facial geometry in standard triangle language (STL) format, compatible with the Autodesk Inventor Professional 2015 software used by Newcastle University School Of Mechanical & Systems Engineering. Scanning was conducted on university premises using a Creaform Go Scan 50TM model. This method was chosen as it allowed working data to be obtained in a small number of brief sessions, appropriate given the limited availability of the volunteer involved and the time constraints placed on this project.



To improve the stability of the STL file when imported into Inventor further processing was carried out to reduce file size and mesh errors. This was initially conducted in MeshLab, a freeware available from ISTI - CNR. The quadric edge collapse decimation faction was used with a progressively lower quality threshold, reducing file size from 3278 KB to 301 KB. Following this, Autodesk NETFABB was used to [remove mesh errors such as duplicate nodes, which cause instability when imported to Inventor. Although this processing resulted in minor resolution loss, the resultant file was significantly improved once imported to CAD when compared to the raw file, with far shorter load times and fewer crashes. Once imported to Inventor and converted into a solid part reference geometry was created in line with the recommendations made by Jensen, et al. These references would serve as datums throughout the development process.<sup>[45]</sup>

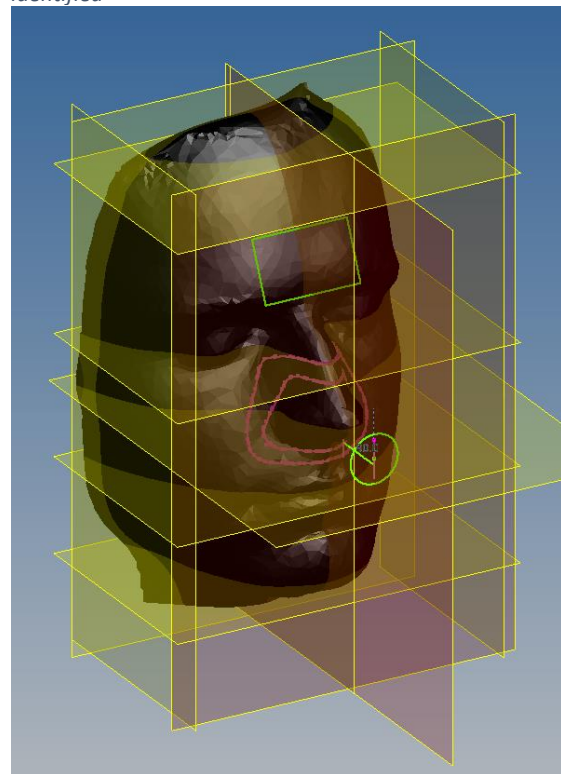
Figure 20: The facial data before and after post processing



## 6.2. Custom CAD model

Following the top down assembly modelling approach proposed by Chen, et al., use was made of the schematics from report section 5.2 'Design Schematics' to establish key geometry, using scan data as the assembly base. The areas around the nasal bridge and nostrils were identified and 2D sketches were projected to the scan surface to create an outline of the mask cushion profile based on the shape of the Eson 2 mask cushion. A work surface was also projected a distance of 15mm from the forehead area to locate where the mask frame would sit with space for the head straps. The frame/elbow junction was modelled a distance of 30mm in front of the nasal tip and 25mm above the masticatory plane to ensure airflow delivery in front of the nasal orifice. In addition, the internal diameter of the hose connection and elbow components were known to be 15mm, as dictated by ISO 17510.<sup>[23]</sup> The skeleton shape of each component was then defined and iteratively improved following the process described by Chen, et al.

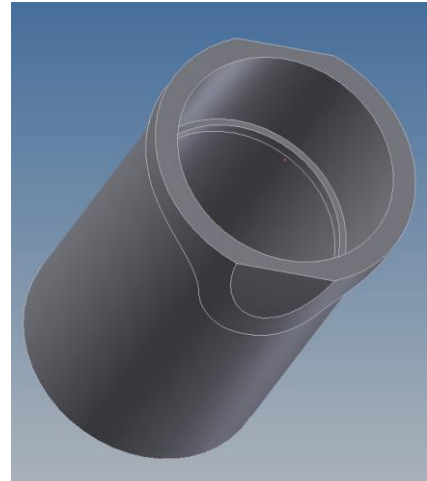
Figure 21: Annotated facial data with key geometry identified



This process was carried out on each part in tandem with use being made of sub-assemblies to simplify development. For example, the complex ball and socket joint between the elbow and frame was left out of the early design stages to avoid complicating the construction of the frame and elbow components respectively. Separate ball and socket parts were made and once the elbow and frame components had been established individual assemblies were created and the ball and socket were mated to their relevant components. These sub-assemblies were then imported into the master assembly, which consisted of five finalised components: the hose connection, elbow, frame, customised mask cushion and the cushion/frame connector.

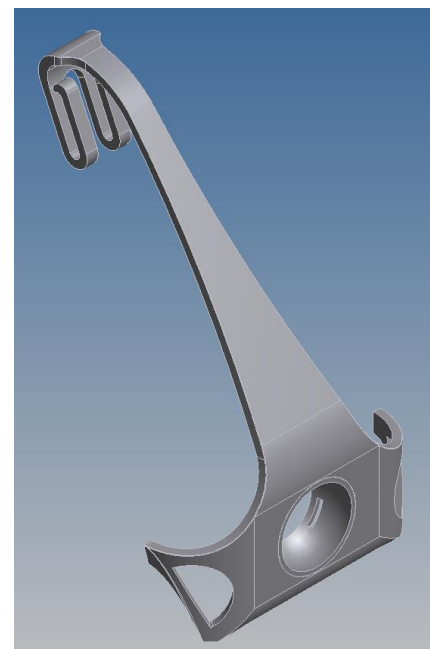
The hose connection links the wider CPAP system and the components reviewed within this CAD model. It is designed with an internal lip which fits into a corresponding recess within the internal face of the elbow tube, shown in Figure 22. This is a common joining method found in CPAP mask models where ease of disassembly is stipulated by ISO 17510. This is further reflected in the design of the outer surface where the component meets the elbow; here a lip with concave indents offers purchase for an operator to exert the force required to disassemble the tube. Of note is the fact that the use of screws and threads is avoided, these features providing small crevices where contaminants may collect. [23]

Figure 22: Hose connector



The protruding end of the elbow component is designed to insert into the hose connector as described, with the other end curving to meet the mask frame. The exhaust port of the Eson 2 model is located on the apex of this curve and is composed of several small circular fixed orifice diffusers. The elbow component ends in a ball which inserts into the socket recess of the frame to create a ball and socket joint. This allows the mask and hose to swivel freely within a range of motion, avoiding restrictions to the wearers freedom of movement.

Figure 23: Frame and joint socket sub assembly



The mask frame is designed to be minimally obtrusive, making use of transparent materials and reducing its shape to areas of key functional geometry, such as the ball and socket joint and connections for fastening head straps. The material between these areas is minimised by the curvature of the frame which avoids obscuring the users line of sight. The design of the Eson 2 uses the head straps to form a cushion against the wearers forehead when secured around the two looped protrusions, as shown in Figure 23, improving security of mask fit whilst avoiding the need for additional cushioning components. A feature developed into this CAD model is the reduction of disruption to airflow when the frame and elbow are in their neutral positions, by the alignment of the socket component overlap with the edge of the interior ball.

The component connecting the frame to the mask cushion is joined by two recess fits on the outer surface of the ball and socket joint, and to the cushion by a silicone seal. This component has a protrusion which inserts into a recess located on the frame, subsequently acting to orient the cushion such that it fits the wearers face. The corresponding functional geometry on the frame is shown in Figure 24. The cushion itself was formed by extruding to the 3D sketch created on the facial scan and its design was influenced by the use of FEA discussed in report section 6.3.

Figure 24: Geometry on socket face used to orientate the mask cushion

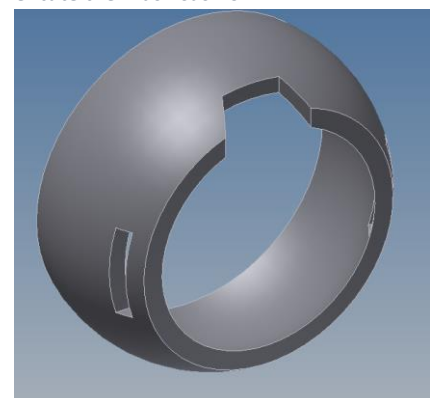
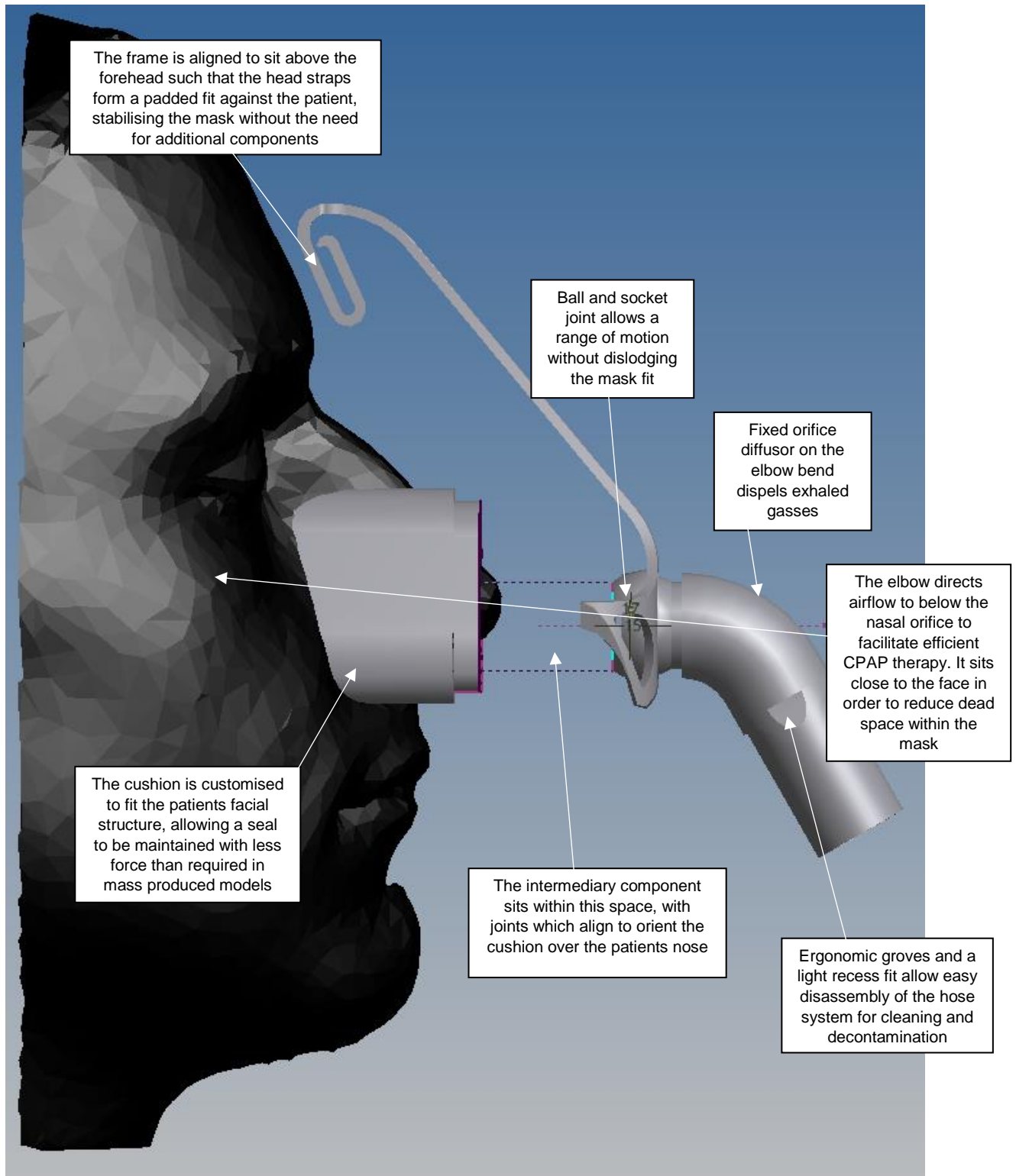


Figure 25: Master assembly with the cushion/frame intermediary removed, with sketch lines to show flow alignment with nasal orifice



### 6.3. Finite Element Analysis (FEA)

Although not the focus of this project, the use of FEA conducted on ANSYS 15.0 Multiphysics Academic Teaching Advanced is included in this section to demonstrate how it can be used to inform CPAP mask design, providing a number of simplifications and assumptions are made.



Head geometry was simplified to a bust of the area immediately surrounding the mask. Ideally this component would have been created by simply filling the scan shell to form a complete solid, but this was not possible within this project due to outdated licenses causing Inventor to crash. Instead this was done manually by picking points on the facial scan and creating splines between rings of points. These splines were then patched and stitched together to create a uniform solid approximating the geometry of the facial scan. To simplify analysis the bust was modelled as a single material assigned the properties of human skin, as listed in Appendices: Item 6. In reality the body is a composite of many different materials, the interactions between which need thorough research for the use of FEA to be truly relevant.<sup>[49]</sup>

Similarly, the interaction between the cushion and wearers face was simplified to one force acting to press the cushion directly into the skin, whereas realistically this would likely be misaligned due to the head straps pulling the mask unevenly. This also neglects the significance of the wearers sleeping position, be it supine or on their side. For the purposes of this study this force was modelled as 10N, following the work of Cheng, et al. in their CPAP related study.<sup>[42]</sup> The parts were in bonded contact with frictionless supports used to keep the two parts aligned and a fixed support under the base of the bust to simulate a surface beneath the wearers head.

Areas of high interest were identified and fitted with an initial face sizing of 1mm, with a coarser 4mm mesh applied elsewhere to reduce calculation times. Assigning the cushion the properties of silicone rubber and solving these initial conditions to find equivalent Von Mises stress gave an answer approximately in line with simple hand calculations, contained in Appendices: Item 7. Following this, mesh convergence was found by incrementally refining the fine mesh sizing until the averaged element equivalent Von Mises stress, calculated by exporting data to excel, was found to be independent of further mesh refinement.

Figure 26: Splines were created from point geometry which were then patched and stitched together to create the functional surface of the bust for use in finite element

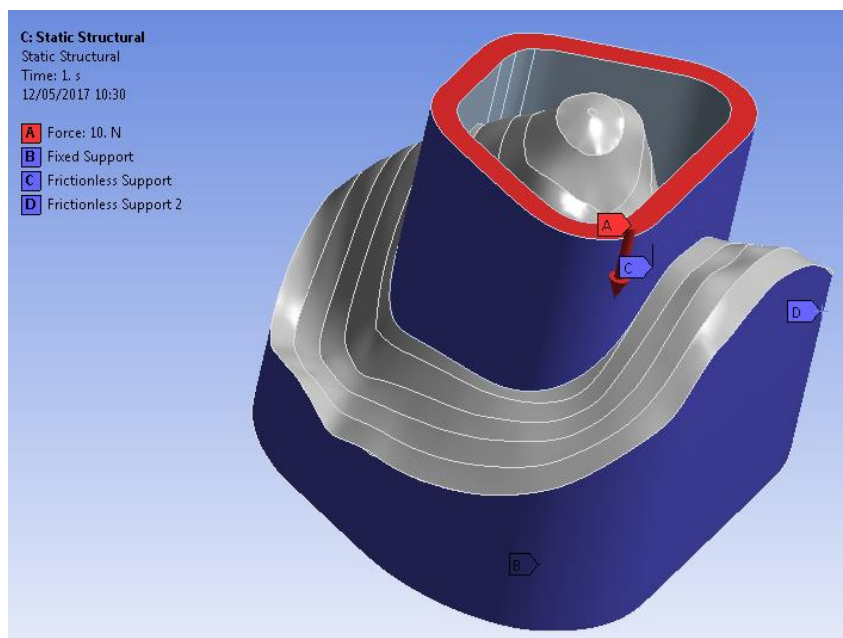
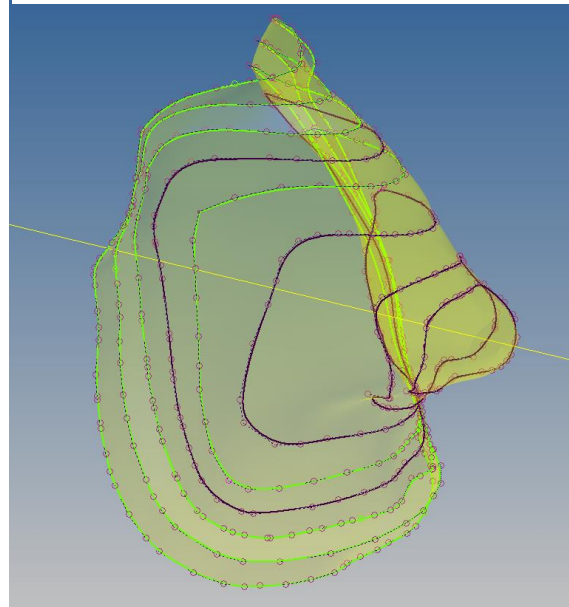


Figure 27: Forces modelled in FEA analysis

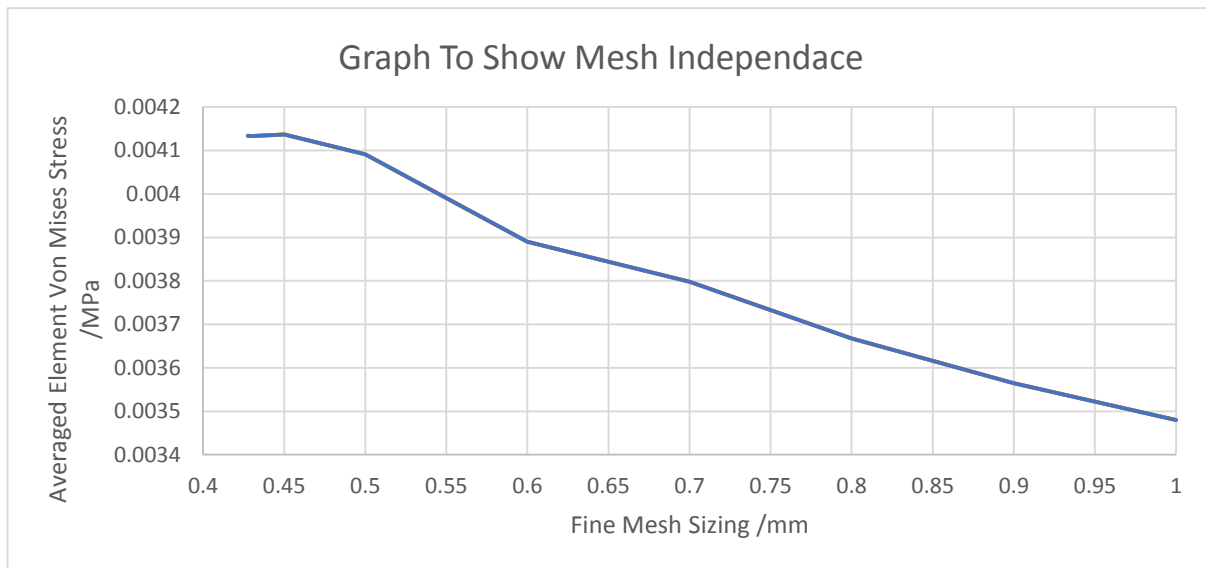


Figure 28: Graph to show mesh independence reached when mesh reduced to 0.45mm

Although no quantitative limits such as the yield or failure of material were investigated, as such specifics would be offset by the large simplifications made in this model, this setup was used to abstractly explore the effects of varying cushion design parameters. For example, the effects of changing the choice of cushion material were investigated. The simulation was run using silicone rubber, natural rubber and silicone elastomer as cushion materials, the results of which are shown in Figures 28, 29 and 30 respectively. It was found that the mean element Von Mises equivalent stress was lowest when the cushion material was silicone rubber, which also resulted in the most favourable stress profile, supporting the established use of this material in commercial masks.

Figure 29: FEA analysis using silicone rubber as the cushion material. Average element equivalent Von Mises stress was 0.004137 MPa. Note how the areas of high stress are more evenly distributed than when other materials are used

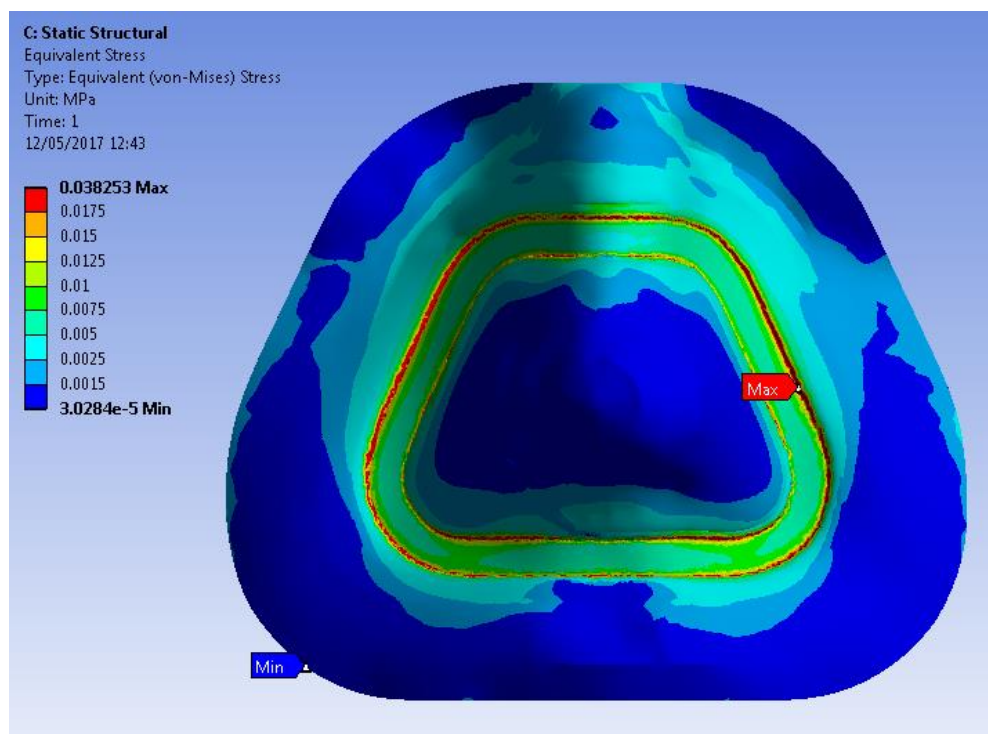




Figure 30: FEA analysis using natural rubber as the cushion material. Average element equivalent Von Mises stress was 0.004244475 MPa

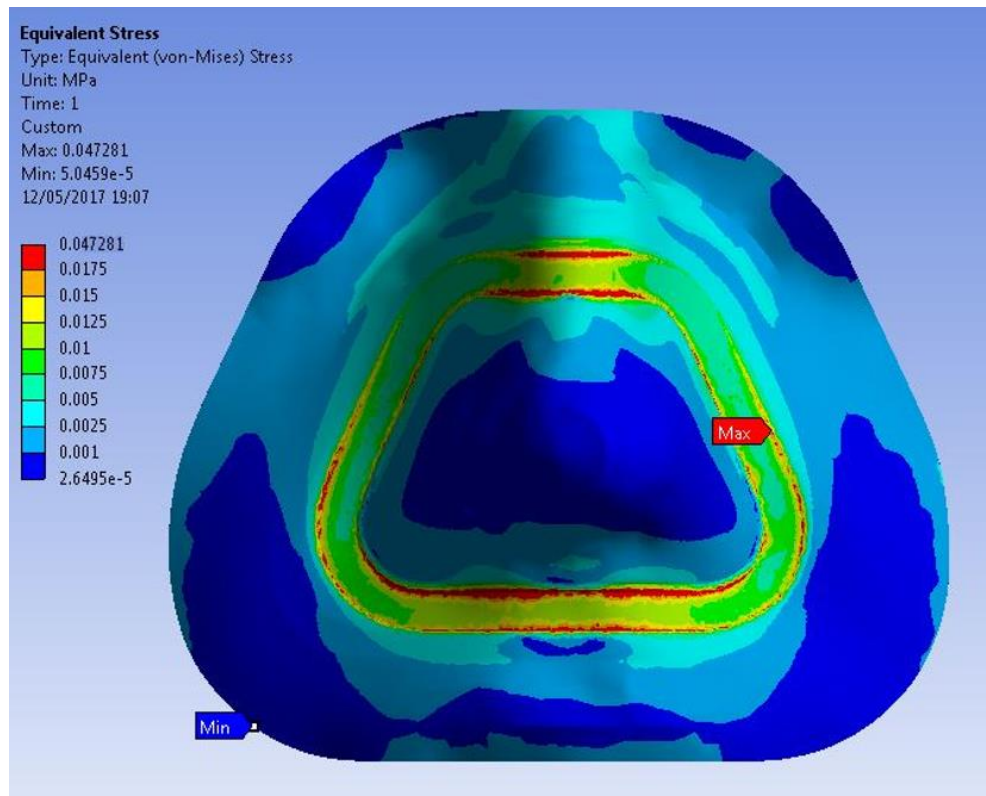
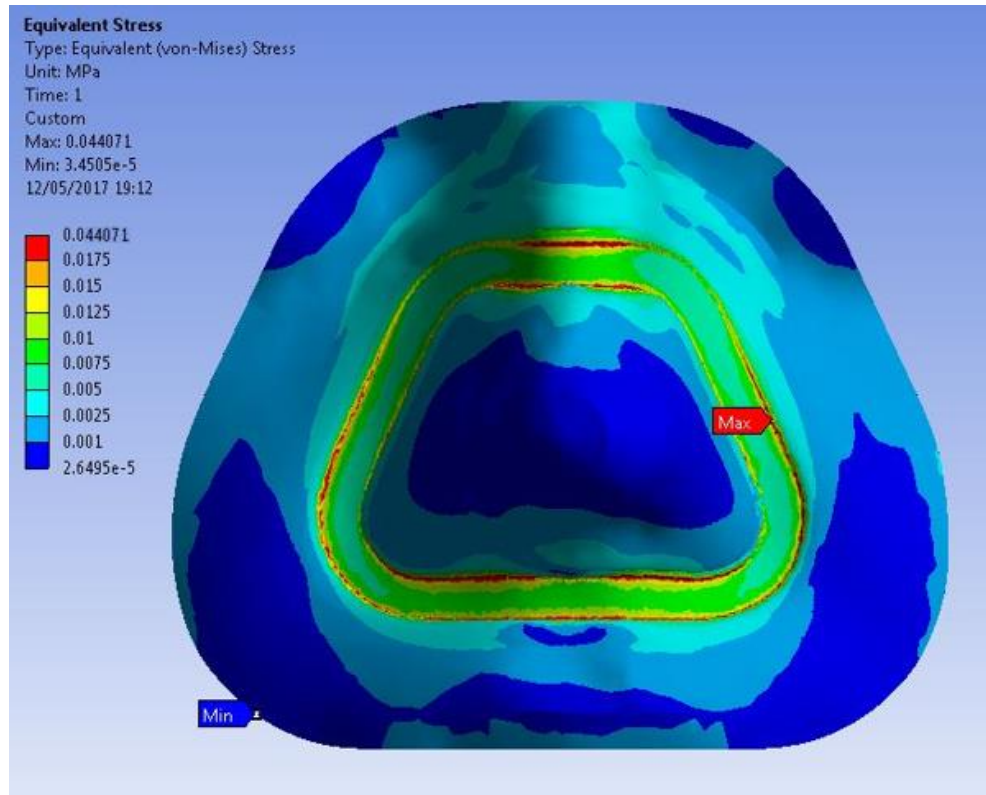


Figure 31: FEA analysis using silicone elastomer as the cushion material. Average element equivalent Von Mises stress was 0.004147926 MPa



## 7. Design Development Discussion & Evaluation

This report section provides a review of the work conducted in report section 6 'Design Development', expanding upon the use of top down assembly modelling and finite element analysis and how these techniques can and are used in the engineering of CPAP masks. Additional review is made of the methods by which mask performance is clinically assessed.

### 7.1. Evaluation Of CPAP Mask Design Methodology

Report section 6 demonstrated the viability of a top down assembly modelling approach and how it can be used in the customisation of articulated biomechanical garments. By identifying geometry key to a chosen CPAP mask design the development process can be simplified; for example the cushion to frame connector component, which would have required prior dimensioning and calculations to form independently, was simply created by lofting between the cushion and frame surfaces to create an intermediary part which was later refined.

This methodology was simple to implement in a one off production process but has the capacity for expansion to mass customisation, theoretically leading to improved compliance due to the discussed benefits of an adapted interface. <sup>[42]</sup> Given a majority of components remain unchanged this could be implemented through modular mask design wherein the bulk mask is produced as standard before being fitted with a unique cushion. Such a production model has successfully been implemented in other industries, with companies like Earcandi producing customised headphone inserts. Earcandi also makes use of medical grade silicone polymers in their product line, the same group of materials commonly found in CPAP masks. <sup>[50]</sup>

Figure 32: Customised headphone inserts by Earcandi



Cheng, et al. separated the cost of producing customised CPAP components into two sections: the fixed capital requirement to attain facial data, design the cushion itself and purchase appropriate rapid tooling or 3D printing equipment, and the variable material cost required to produce components. As technology continues to develop it is expected that these associated fixed costs will decrease. Customization itself becomes more viable when multiple cushions are produced at once, this being a relevant consideration given it is recommended for users to replace CPAP mask cushions every six months. Example economies of scale are demonstrated in Appendices: Item 9. <sup>[42]</sup>

Within this project it was found that the computing power and stability of software used limits the ability to accurately customise components. Personal experience encountered frequent crashing and inability of Autodesk Inventor Professional 2015 to carry out certain functions, but it can be expected that such issues would not be as limiting in a contemporary industrial setting. It is recommended that the base scan data is obtained in the highest resolution possible as this can later be reduced in



Figure 33: Facial scan data taken from a realistic infant doll for the intent of developing a neonatal CPAP mask

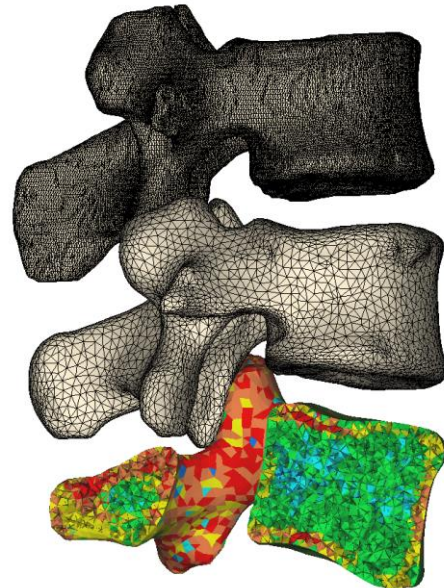
complexity using post processing software, as necessitated by the program and computer combination used in the design process.

Further demonstration of a top down assembly modelling approach to the design of a neonatal CPAP mask was originally planned, facial data being obtained from a realistic model, but was curtailed due to time constraints.

Figure 34: Spinal vertebrae made in MIMICS, displaying various mesh configurations

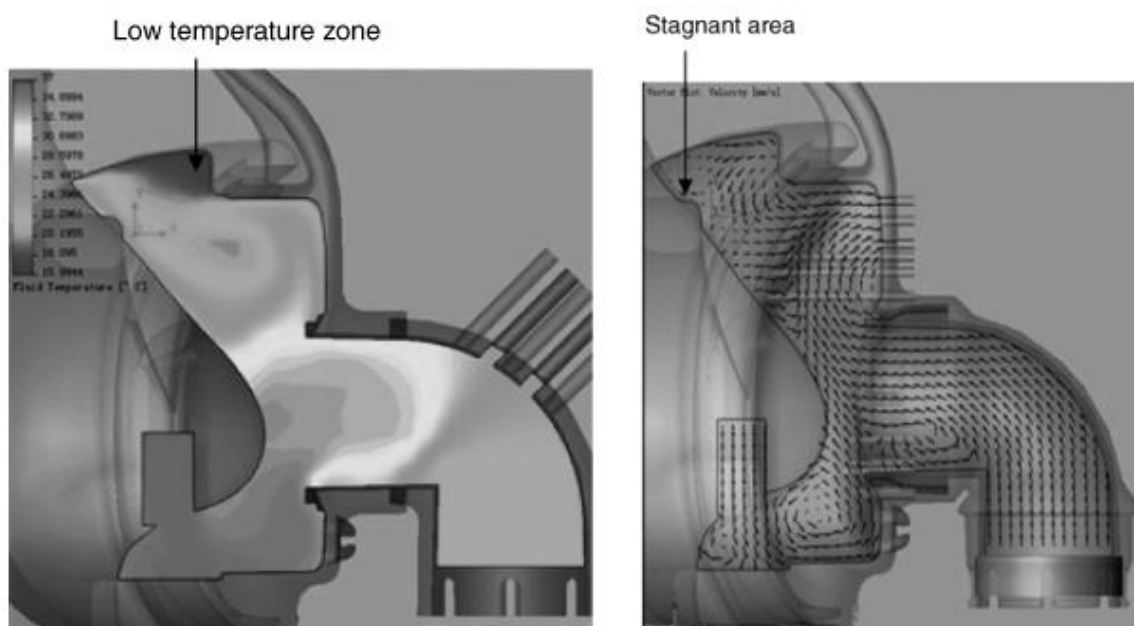
## 7.2. Further use of computational modelling

To facilitate realistic analysis of aspects such as deformation and material wear, the FEA model demonstrated in report section 6.3 'Finite Element Analysis (FEA)' would need to be increased in complexity. Sophisticated application of FEA is particularly relevant in mass produced CPAP masks where the mask seal is formed by the deformation of excess material as it is pressed into the wearers face. A different example of how the model could be improved would be the use of specialised CAD programs, such as Materialise Interactive Medical Image Control System (MIMICS), to accurately model bio material. Such models could be used in conjunction with 3Matic, a program designed to create meshes from anatomical data. <sup>[51][52]</sup>



An important application of FEA software to CPAP mask design is fluid modelling for use in the evaluation of flow dynamics and condensation formation. An example would be the plotting of temperature distribution and air velocity within a mask to identify areas of hot stagnant air where condensates would be likely to precipitate on the lower temperature mask surface. Such analysis is especially pertinent to customised masks as geometric alteration will affect flow dynamics compared to those found in standard issue models. <sup>[37][41]</sup>

Figure 35: FEA can be used in a range of applications, such as creating temperature and velocity plots to identify probable areas of condensation formation



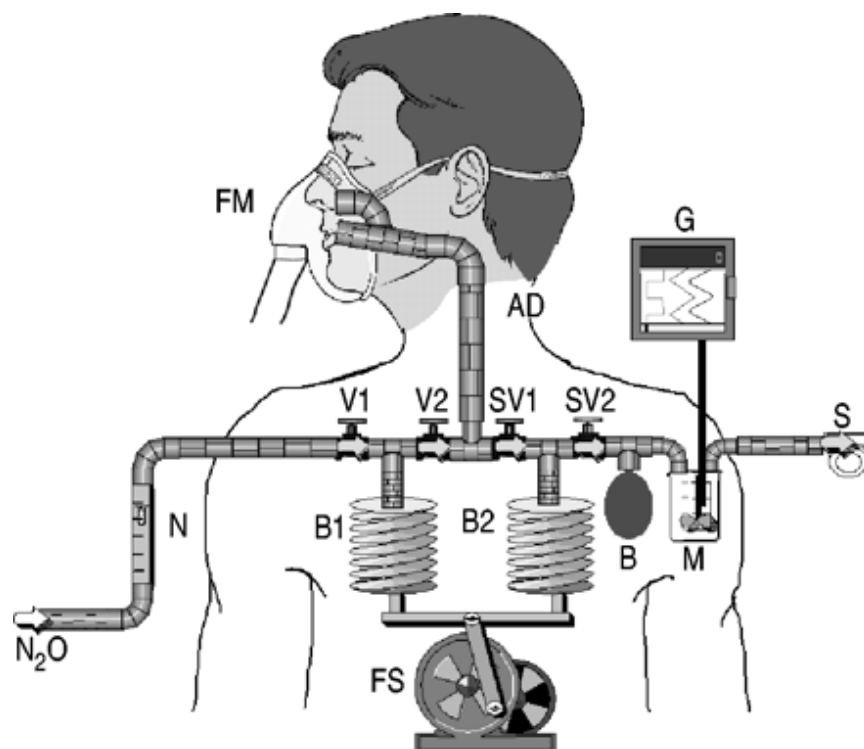


### 7.3. Assessing CPAP Mask Performance

As with all medical devices astute evaluation and review of device performance is critical to allow continued improvements in the field of healthcare. CPAP manufacturers often make use of patient feedback, each with their own associated infrastructures and support networks set up on line. Such patient feedback is useful but mostly qualitative in nature. Evaluation of mask performance in a clinical setting offers greater advantages, with substantial medical literature dedicated to the assessment of OSA severity. Such literature lays a standardised framework within which to assess patient improvements brought about through mask use. Techniques often used to assess CPAP mask performance are the recording of apnoea and hypopnea indices, oxyhemoglobin saturation and polysomnographic records.<sup>[16]</sup>

The development of realistic breathing simulators has allowed for real time mask performance evaluation without test subjects being placed at risk. Experimental set ups such as that used by Saatchi, et al. in Figure 34 allow monitoring of gaseous profiles and pressure swings, used to assess a masks capacity to vent and maintain a seal under different pressures.<sup>[41]</sup> Similarly it is also possible to use particle counting devices to quantify particle concentrations within a mask compared to a laboratory ambient in order to evaluate fit and seal quality.<sup>[42]</sup> Additional tests used to ratify mask performance are outlined in the appendices of ISO 17510.<sup>[23]</sup>

Figure 36: A lung simulator with various component labelled such as face mask (FM) and anatomical deadspace (AD)



## 8. Developing CPAP Mask Concepts

As described in report section 4.1 ‘CO<sub>2</sub> Rebreathing Reduction’, the optimisation of CPAP masks is limited as the bias flow rate of mass produced masks must be over-engineered to accommodate for users whose prescribed therapy utilises the lower range of pressures. Recent developments have attempted to address this issue by creating non fixed diffusers, where patients receiving high pressure airflow have the capacity to reduce bias flow rate and therefore machine noise and pressure swings.<sup>[37]</sup> Manufacturers such as Fischer & Paykel

have recently begun producing porous overlays which clip over the fixed orifices to disrupt flow dynamics and reduce the efficiency of the unnecessarily over performing diffuser. Data taken from the user manual of the Eson 2 shows the flow characteristics both with and without said attachment, shown in Figure 37, illustrating how these devices can be used to modulate mass produced masks to suit a patients operating pressure.<sup>[53]</sup>

An alternative approach is to create orifices with the capacity to change their cross sectional area, following the parameters of the calculations identified in section 4.1. Currently there are no commercial models with this function, but concepts such as that developed by Zhen, et al. demonstrate how this could hypothetically be approached. The difficulty however arises regarding how this cross sectional area will be finely controlled to accommodate for fluctuations in the pressure of supplied airflow.<sup>[37]</sup>

Pressure (cmH <sub>2</sub> O)	4	6	8	10	12	14	16	18	20	22	24	26	28	30
Flow with Diffuser (L/min)	19	25	29	34	38	41	45	48	52	55	58	61	63	66
Flow without Diffuser (L/min)	27	34	39	44	48	52	56	59	62	66	69	71	74	77

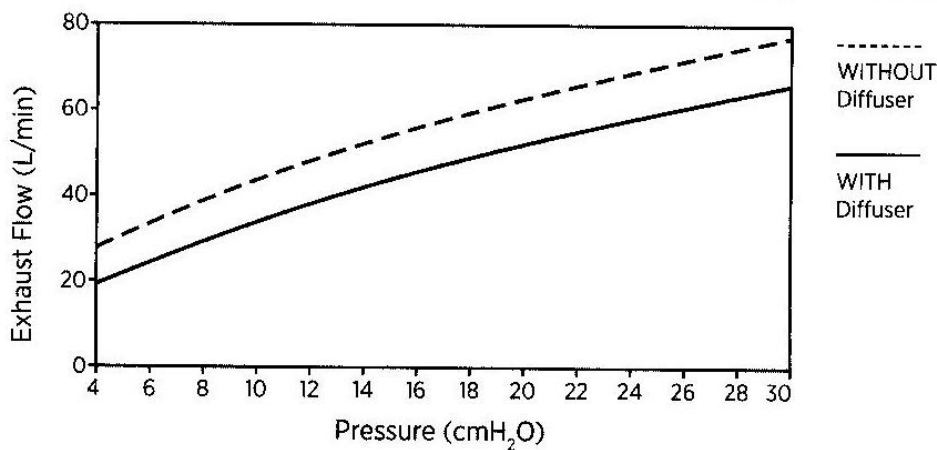


Figure 38 Flow characteristic of the Eson 2, with and without the attachment

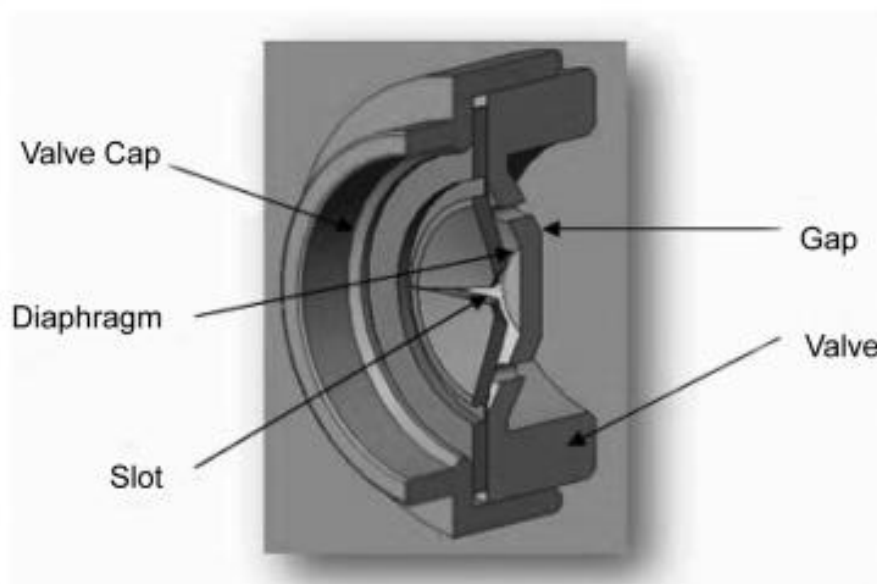


Figure 39: Concept of a variable diffuser design



An additional area of research being undertaken is in masks which eliminate skin contact, avoiding dermal irritation and injury. An example is the head helmet design shown in Figure 39.

An exploratory study by Patroniti, et al. came to the conclusion that such a model can be used in a successful CPAP system, but there is limited supporting literature available and such designs have yet to be made commercial.<sup>[54]</sup>

A potential idea discussed with supervisors over the course of this project was the potential for CPAP masks to have transitioning cushion areas, which could be implemented through a bi-valve pressure system controlled by a solenoid. Should such a concept be implemented the potential benefits would be two fold, the periodic removal of stress reducing skin damage and also allowing brief aeration.



Figure 40: CPAP head helmet design

## 9. Conclusion

This project has successfully conducted an in-depth exploration of the engineering behind CPAP masks, ranging from commercial model evaluation and material choice to a review of the design parameters critical to the production of successful masks. A simple mechanism by which to assess mask appropriateness for given patient was also developed and discussed in report section 3.2. The context of CPAP mask use was thoroughly established and an in depth review was undertaken of considerations unique to CPAP mask engineering. Analysis was made of the factors limiting mask optimisation, such as ISO 17510 specifying that all masks must operate at pressures as low as 4 cm H<sub>2</sub>O regardless of intended use. From this it was inferred that masks characteristics such as bias flow rate are over engineered, resulting in performance loss in terms of certain aspects such as machine noise. Having identified a need for improved customisability an investigation was undertaken into how top down assembly modelling can be implemented to facilitate adaptation of the patient/mask interface, successfully adapting the geometry of the Eson 2 Nasal Mask to digitized facial data.

Practical work conducted was successful within the context of this project, furthering the Author of this reports comprehension and understanding of the design methodologies and processes which can be applied to complex medical products such as CPAP masks. Although brief, finite element analysis supported the trend of manufacturers to use silicone as the mask cushion material of choice, its use resulting in the lowest average element equivalent Von Mises stress compared to other materials. Visual inspection also observed a superior stress profile, the silicone cushion evenly distributing force compared to the natural rubber and silicone elastomer comparisons simulated.

This work allowed assessment of top down assembly modelling as a viable design addition, supported by contextual research into how customisability could be implemented to a greater extent in industry, such as identifying fixed and variable costs related to product customisation.

Mathematical parameters identified at the research stage, such as the effect of orifice shape and size on mask bias flow rate, were used to later identify developing concepts which could lead to improved patient compliance, such as the use of variable orifice diffusors.

The main deliverable of this project was achieved in the form of the comprehensive review detailed in this report, with the outline for future work being established.

## 10. Future Work

---

Due to time constraints it was not possible to pursue the development of a neonatal CAD model, despite research into this area being conducted in the early stages of this project. Should time have allowed, this avenue of research would have been pursued in order to see how the design methodology compares and contrasts with that described in report section 6.

Future work would look to explore how the models used in FEA can be expanded to investigate the effects altering mask design has on the fluid behaviour within the mask. The scope for this future work is vast, but would require competencies with programmes such as FLUENT to a level the Author of this report does not currently possess. A potential area for focus could be the varying of the thermal resistance provided by the mask and the effect this has on condensation formation. This could be investigated by varying parameters such as mask wall thickness or selecting materials with different thermal characteristics. Additionally, if time had allowed, this project intended to go on to evaluate in depth the manufacture and production of customised components and how rapid tooling and 3D printing can be used. This could culminate in the production of one or more prototypes, allowing physical evaluation of the personalised mask cushion designed.

## 11. References

---

### Text references:

- [1] Scribd. (2017). *IVMS| Textbook of Human Physiology and Biophysics | Homeostasis | Respiratory System*. [online] Available at: <https://www.scribd.com/doc/200697780/IVMS-Textbook-of-Human-Physiology-and-Biophysics> [Accessed 14 May 2017].
- [2] Waugh, J. (2006). *Trends in Noninvasive Respiratory Support: Continuum of Care*. 1st ed. [ebook] Saxe Healthcare Communications, p.7. Available at: <http://www.clinicalfoundations.org/assets/foundations3.pdf> [Accessed 14 May 2017].
- [3] Sanders, M., Kern, N., Stiller, R., Strollo, P., Martin, T. and Atwood, C. (1994). CPAP Therapy via Oronasal Mask for Obstructive Sleep Apnoea. *Chest*, 106(3), pp.774-779.
- [4] Newhouse, T., et al. (1994) Hospital-based Asthma Education: Achieving the Goals and Evaluating the Outcome, *Chest*, Vol.84, pp.712-715 [Peer Reviewed Journal]
- [5] Nave, R. (2017). *Pressure*. [online] Hyperphysics.phy-astr.gsu.edu. Available at: <http://hyperphysics.phy-astr.gsu.edu/hbase/ptens3.html> [Accessed 14 May 2017].
- [6] Basford, J. (2002). The Law of Laplace and its relevance to contemporary medicine and rehabilitation. *Archives of Physical Medicine and Rehabilitation*, 83(8), pp.1165-1170.
- [7] Doyle, D F. (2017), personal correspondence
- [8] Barrowcliffe, M. (1986). PEEP and CPAP. *BMJ*, 292(6527), pp.1077-1077.
- [9] Mechanisms of the Effectiveness of Continuous Positive Airway Pressure in Obstructive Sleep Apnoea. (1992). *Sleep*, (356), pp.1751–1758.
- [10] Al-Jumaily, A. and Reddy, P. (2012). *Medical devices for respiratory dysfunction*. 1st ed. New York, NY: ASME Press, Chapter 1.
- [11] Stockman, J. (2012). Nasal continuous positive airway pressure (CPAP) versus bi-level nasal CPAP in preterm babies with respiratory distress syndrome: a randomised control trial. *Yearbook of Pediatrics*, 2012, pp.422-423.

- [12] Sanders, M.H. and Kern, N., 1990, Obstructive sleep apnoea treated by independently adjusted inspiratory and expiratory positive airway pressures via nasal mask: physiologic and clinical implications, *Chest*, 98(2), p. p317(8).
- [13] Robertson, A. (2003). Reflections on Errors in Neonatology: II. The “Heroic” Years, 1950 to 1970. *Journal of Perinatology*, 23(2), pp.154-161.
- [14] Marketsandmarkets.com. (2017). *Sleep Apnoea Devices Market by Product, Diagnostic, Therapeutic & End User - 2021 | MarketsandMarkets*. [online] Available at: <http://www.marketsandmarkets.com/Market-Reports/sleep-apnoea-devices-market-719.html> [Accessed 14 May 2017].
- [15] Maximintegrated.com. (2017). *How Continuous Positive Airway Pressure (CPAP) Respiratory Ventilation Systems Function - Tutorial - Maxim*. [online] Available at: <https://www.maximintegrated.com/en/app-notes/index.mvp/id/4685> [Accessed 14 May 2017].
- [16] Jones, D., Braid, G. and Wedzicha, J. (1994). Nasal masks for domiciliary positive pressure ventilation: patient usage and complications. *Thorax*, 49(8), pp.811-812.
- [17] Douglas, N. (1998). Systematic review of the efficacy of nasal CPAP. *Thorax*, 53(5), pp.414-415.
- [18] P.S.Dhami; G.Chopra; H.N. Shrivastava (2015). *A Textbook of Biology. Jalandhar, Punjab: Pradeep Publications. pp. V/101.*
- [19] Langford, N. (2005). Carbon Dioxide Poisoning. *Toxicological Reviews*, 24(4), pp.229-235.
- [20] Farré, R., Montserrat, J., Ballester, E. and Navajas, D. (2002). Potential Rebreathing After Continuous Positive Airway Pressure Failure During Sleep. *Chest*, 121(1), pp.196-200.
- [21] Nilius, G., Domanski, U., Franke, K. and Ruhle, K. (2008). Impact of a controlled heated breathing tube humidifier on sleep quality during CPAP therapy in a cool sleeping environment. *European Respiratory Journal*, 31(4), pp.830-836.
- [22] Bacon JP, Farney RJ, Jensen RL, Walker JM, Cloward TV. *Nasal continuous positive airway pressure devices do not maintain the set pressure dynamically when tested under simulated clinical conditions. Chest* 2000;118:1441–1449
- [23] BS EN ISO 17510-2:2009. (2017). 1st ed. [ebook] BSOL Standards Online. Available at: <https://bsol.bsigroup.com/Bibliographic/BibliographicInfoData/000000000030192481> [Accessed 14 May 2017].
- [24] BS EN ISO 10993-10:2010. (2017). 1st ed. [ebook] BSOL Standards Online. Available at: <https://bsol.bsigroup.com/Bibliographic/BibliographicInfoData/000000000030263004> [Accessed 14 May 2017].
- [25] Eu-pap.co.uk. (2017). *Types of CPAP masks | EU-PAP*. [online] Available at: <http://www.eu-pap.co.uk/mask-types> [Accessed 14 May 2017].
- [26] Partinen, M. and Telakivi, T. (1992). Epidemiology of Obstructive Sleep Apnoea Syndrome. *Sleep*, 15(suppl\_6), pp.S1-S4.
- [27] Anon, (2017). *Chronic Respiratory Diseases*. [online] Available at: [http://www.who.int/gard/publications/chronic\\_respiratory\\_diseases.pdf](http://www.who.int/gard/publications/chronic_respiratory_diseases.pdf) [Accessed 14 May 2017].

- [28] Buettiker, V., Hug, M., Baenziger, O., Meyer, C. and Frey, B. (2004). Advantages and disadvantages of different nasal CPAP systems in newborns. *Intensive Care Medicine*, 30(5), pp.926-930.
- [29] Manssor, N., Radzi, Z., Yahya, N., Mohamad Yusof, L., Hariri, F., Khairuddin, N., Abu Kasim, N. and Czernuszka, J. (2016). Characteristics and Young's Modulus of Collagen Fibrils from Expanded Skin Using Anisotropic Controlled Rate Self-Inflating Tissue Expander. *Skin Pharmacology and Physiology*, 29(2), pp.55-62.
- [30] Jeon, G. (2016). Respiratory support with heated humidified high flow nasal cannula in preterm infants. *Korean Journal of Pediatrics*, 59(10), p.389.
- [31] Polycarbonate, EduPack. (2016). CES.
- [32] Silicone, EduPack. (2016). CES.
- [33] Stücker, M., Struk, A., Altmeyer, P., Herde, M., Baumgärtl, H. and Lübbers, D. (2002). The cutaneous uptake of atmospheric oxygen contributes significantly to the oxygen supply of human dermis and epidermis. *The Journal of Physiology*, 538(3), pp.985-994.
- [34] Polyurethane, EduPack. (2016). CES.
- [35] Samolski, D., Calaf, N., Güell, R., Casan, P. and Antón, A. (2016). Carbon dioxide rebreathing in non-invasive ventilation. Analysis of masks, expiratory ports and ventilatory modes. *Monaldi Archives for Chest Disease*, 70(3).
- [36] Zetterström, H. and Jonsson, L. (1987). Pressure characteristics of the Ambu CPAP system and the Servo Ventilator 900C in CPAP mode. *Acta Anaesthesiologica Scandinavica*, 31(1), pp.104-110.
- [37] Al-Jumaily, A. and Reddy, P. (2012). *Medical devices for respiratory dysfunction*. 1st ed. New York, NY: ASME Press, Chapter 6.
- [38] Al-Jumaily, A. and Reddy, P. (2012). *Medical devices for respiratory dysfunction*. 1st ed. New York, NY: ASME Press, Chapter 3.
- [39] Wu, D., *Analysis and Simulation of LSPC Hydraulic Systems*, 2003, University of Saskatchewan, Saskatoon.
- [40] Schettino, G., Chatmongkolchart, S., Hess, D. and Kacmarek, R. (2003). Position of exhalation port and mask design affect CO<sub>2</sub> rebreathing during noninvasive positive pressure ventilation\*. *Critical Care Medicine*, 31(8), pp.2178-2182.
- [41] Saatci, E., Miller, D., Stell, I., Lee, K. and Moxham, J. (2004). Dynamic dead space in face masks used with noninvasive ventilators: a lung model study. *European Respiratory Journal*, 23(1), pp.129-135.
- [42] Cheng, Y. and Chu, J. (2013). Application of rapid tooling to manufacture customized nasal mask cushion for continuous positive airway pressure (CPAP) devices. *Rapid Prototyping Journal*, 19(1), pp.4-10.
- [43] Personalized 3D-Printed CPAP Masks Improve CPAP Effectiveness. (2014). 1st ed. [ebook] University Of Michigan. Available at: <http://www.researchposters.com/Posters/COSM/COSM2015/H118.pdf> [Accessed 14 May 2017].

[44] Wei, Y., Li-Tsang, C., Liu, J., Xie, L. and Yue, S. (2017). 3D-printed transparent facemasks in the treatment of facial hypertrophic scars of young children with burns. *Burns*, 43(3), pp.e19-e26.

[45]

[46] Chen, X., Gao, S., Yang, Y. and Zhang, S. (2012). Multi-level assembly model for top-down design of mechanical products. *Computer-Aided Design*, 44(10), pp.1033-1048.

[47] Logbook 1, pp157-158

[48] Logbook 1, pp32-39

[49] Saraf, H., Ramesh, K., Lennon, A., Merkle, A. and Roberts, J. (2007). Mechanical properties of soft human tissues under dynamic loading. *Journal of Biomechanics*, 40(9), pp.1960-1967.

[50] Earcandi. (2017). *Earcandi - Custom earphones and earplugs | Home*. [online] Available at: <https://earcandi.com/> [Accessed 14 May 2017].

[51] Materialise. (2017). Mimics. [online] Available at: <http://www.materialise.com/en/medical/software/mimics> [Accessed 14 May 2017].

[52] Materialise. (2017). Software. [online] Available at: <http://www.materialise.com/en/software> [Accessed 14 May 2017].

[53] Eson 2 Nasal Mask Use & Care Guide. (2017). 1st ed. Fischer & Paykel Healthcare, p.8.

[54] Taccone, P. and Chiumello, D. (2016). Face Mask vs Helmet for Noninvasive Ventilation. *JAMA*, 316(14), p.1496.

### Figure References:

Figure 1: Cpap.com. (2017). *ComfortFull 2 Full Face CPAP Mask with Headgear | CPAP.com*. [online] Available at: <https://www.cpap.com/productpage/comfortfull-2-full-face-cpap-mask-with-headgear.html> [Accessed 14 May 2017].

Figure 2: Victoria, C. (2017). *Eliminate the Side Effects of CPAP Therapy | CPAP Victoria Blog*. [online] Cpapvictoria.com.au. Available at: <https://cpapvictoria.com.au/blog/cpap/eliminate-side-effects-cpap-therapy/> [Accessed 14 May 2017].

Figure 3: Text reference 6

Figure 4: Text reference 6

Figure 5: Text reference 13

Figure 6: Text reference 9

Figure 7: Anon, (2017). [online] Available at: <http://pixgood.com/nasopharynx-anatomy.html> [Accessed 14 May 2017].

Figure 8: Leelawong, M. and Holland, A. (2017). *Neonatal Nasal CPAP Device Redesign*. 1st ed. [ebook] Department of Biomedical Engineering, Vanderbilt University. Available at: <http://research.vuse.vanderbilt.edu/srdesign/2003/group14/BME%20273%20-%20Final%20Paper.pdf> [Accessed 14 May 2017].



Figure 9: Text reference 23

Figure 10: Text reference 38

Figure 11: Text reference 37

Figure 12: Text reference 41

Figure 13: Replacement, E. (2017). *EasyFit SilkGel CPAP Nasal Mask Cushion Replacement*. [online] Respsshop - Cheapest CPAP Machines & Supplies. Available at: <https://www.respsshop.com/cushions-nasal-cpap-mask/easyfit-silkgel-replacement-p-744.html> [Accessed 14 May 2017].

Figure 14: Text reference 16

Figure 15: Text reference 43

Figure 16: Text reference 45

Figure 17: Text reference 45

Figure 18: Text reference 46

Figures 19-31: Original content

Figure 32: Earcandi. (2017). *Earcandi - Custom earphones and earplugs | Home*. [online] Available at: <https://earcandi.com/> [Accessed 14 May 2017].

Figure 33: Original content

Figure 34: En.wikipedia.org. (2017). *Mimics*. [online] Available at: <https://en.wikipedia.org/wiki/Mimics> [Accessed 14 May 2017]. Figure 35: Text reference 45

Figure 35: Text reference 37

Figure 36: Text reference 41

Figure 37: Text reference 53

Figure 38: Text reference 37

Figure 39: Cpaptalk.com. (2017). *CPAP Community - View topic - Leaks*. [online] Available at: <http://www.cpaptalk.com/viewtopic/p1059823/Leaks.html> [Accessed 14 May 2017].

### Table references:

Table 1: Original content

Table 2: CHRONIC RESPIRATORY Diseases. (2017). 1st ed. [ebook] World Health Organisation, p.33. Available at: [http://www.who.int/gard/publications/chronic\\_respiratory\\_diseases.pdf](http://www.who.int/gard/publications/chronic_respiratory_diseases.pdf) [Accessed 14 May 2017].

Table 3: Original content

Table 4: Fisherpaykel.com. (2017). *Kitchen & Laundry Appliances - Fisher & Paykel US*. [online] Available at: <https://www.fisherpaykel.com/us.html> [Accessed 14 May 2017].

## 12. Appendices

### Item 1: Expanded Manufacturers List Of Materials

#### FlexiFit™ 407

Component	Material
Mask Base	Polycarbonate (PC)
Elbow	Polycarbonate (PC)
Swivel	Polycarbonate (PC)
Silicone Seal	Silicone (LSR)
Forehead Cushion	Silicone (LSR)
Foam Cushion	Polyurethane foam
Glider™ Strap	Nylon (PA)
Stretchgear™ Headgear	Breathe-o-prene™ (Lycra™ / Polyurethane foam laminate)
Pressure Ports Connector (Euro Only)	Polycarbonate (PC) / Santoprene™ (TPE)

#### Quattro™ FX Full Face Mask / Quattro™ FX Non-Vented Full Face Mask

Component	Material
Frame	Polycarbonate
Swivel	15% PTFE in Polycarbonate
Elbow	Polycarbonate (NV has blue tint)
Headgear Clip	Polyester (PBT)
Ports Cap	Silicone Elastomer
Mask Cushion	Silicone Elastomer
Valve	Silicone Elastomer
Valve Clip	Polycarbonate
Headgear	<i>Foam Layer:</i> Open cell Polyurethane <i>Loop Material:</i> Nylon/Spandex <i>Underside Fabric:</i> Nylon/Spandex <i>Fastener Tabs:</i> Polycaprolactam (Polyamide Family) <i>Cloth Label:</i> Rayon acetate satin
Soft Sleeves	88% Nylon / 12% Spandex

#### FullLife

Frame	Thermoplastic polyester elastomer
Outer flap (SST)	Silicone
Entrainment elbow and swivel	Polycarbonate
Elbow split washer	Polycarbonate
Entrainment valve flapper	Silicone
Headgear	UBL/Urethane foam/Lycra and nylon

## Item 2: Polycarbonate Material Properties (EduPack)<sup>[31]</sup>

### Bio-data

Biocompatible	(i)	✓
Medical grades	(i)	✓

### General properties

Density	(i)	1.14e3	-	1.21e3	kg/(m <sup>3</sup> )
Price	(i)	* 2.62	-	2.85	GBP/kg

### Mechanical properties

Young's modulus	(i)	2	-	2.44	GPa
Shear modulus	(i)	0.789	-	0.872	GPa
Bulk modulus	(i)	3.7	-	3.9	GPa
Poisson's ratio	(i)	0.391	-	0.408	
Yield strength (elastic limit)	(i)	59	-	70	MPa
Tensile strength	(i)	60	-	72.4	MPa
Compressive strength	(i)	69	-	86.9	MPa
Elongation	(i)	70	-	150	% strain
Hardness - Vickers	(i)	17.7	-	21.7	HV
Fatigue strength at 10 <sup>7</sup> cycles	(i)	22.1	-	30.8	MPa
Fracture toughness	(i)	2.1	-	4.6	MPa*m <sup>(1/2)</sup>
Mechanical loss coefficient (tan delta)	(i)	0.0164	-	0.0181	

### Optical properties

Transparency	(i)	Optical Quality
Refractive index	(i)	1.54 - 1.59

### Processability

Castability	(i)	1	-	2
Moldability	(i)	4	-	5
Machinability	(i)	3	-	4
Weldability	(i)	5		

## Item 3: Silicone Material Properties (Edupack)<sup>[32]</sup>

### Bio-data

Biocompatible	(i)	✓
Medical grades	(i)	✓

### General properties

Density	(i)	1.3e3	-	1.55e3	kg/(m <sup>3</sup> )
Price	(i)	* 7.37	-	8.77	GBP/kg
Biomaterial	(i)	✓			
Biomedical material	(i)	✓			

### Mechanical properties

Young's modulus	(i)	0.008	-	0.03	GPa
Shear modulus	(i)	* 0.003	-	0.01	GPa
Bulk modulus	(i)	* 2	-	2.2	GPa
Poisson's ratio	(i)	* 0.498	-	0.5	
Yield strength (elastic limit)	(i)	* 5.4	-	7	MPa
Tensile strength	(i)	5.4	-	7	MPa
Compressive strength	(i)	* 10	-	30	MPa
Elongation	(i)	450	-	530	% strain
Fatigue strength at 10 <sup>7</sup> cycles	(i)	* 5	-	6	MPa
Flexural modulus	(i)	* 0.008	-	0.03	GPa
Flexural strength (modulus of rupture)	(i)	5.4	-	7	MPa
Fracture toughness	(i)	* 0.4	-	0.7	MPa*m <sup>(1/2)</sup>
Mechanical loss coefficient (tan delta)	(i)	* 0.4	-	0.9	

### Optical properties

Transparency	(i)	Transparent
Refractive index	(i)	1.4 - 1.44

#### Item 4: Polyurethane Material Properties (EduPack)<sup>[33]</sup>

##### Bio-data

Biocompatible	①	✓
Medical grades	①	✓

##### General properties

Density	①	1.02e3	-	1.25e3	kg/(m <sup>3</sup> )
Price	①	* 3.51	-	4.21	GBP/kg
Date first used	①	1941			
Biomaterial	①	✓			
Biomedical material	①	✓			

##### Mechanical properties

Young's modulus	①	0.002	-	0.03	GPa
Shear modulus	①	7e-4	-	0.008	GPa
Bulk modulus	①	1.5	-	1.6	GPa
Poisson's ratio	①	0.49	-	0.498	
Yield strength (elastic limit)	①	25	-	51	MPa
Tensile strength	①	25	-	51	MPa
Compressive strength	①	50	-	100	MPa
Elongation	①	380	-	720	% strain
Fatigue strength at 10 <sup>7</sup> cycles	①	* 18.8	-	38.3	MPa
Fracture toughness	①	0.2	-	0.4	MPa*m <sup>1/2</sup>
Mechanical loss coefficient (tan delta)	①	* 0.51	-	1.2	

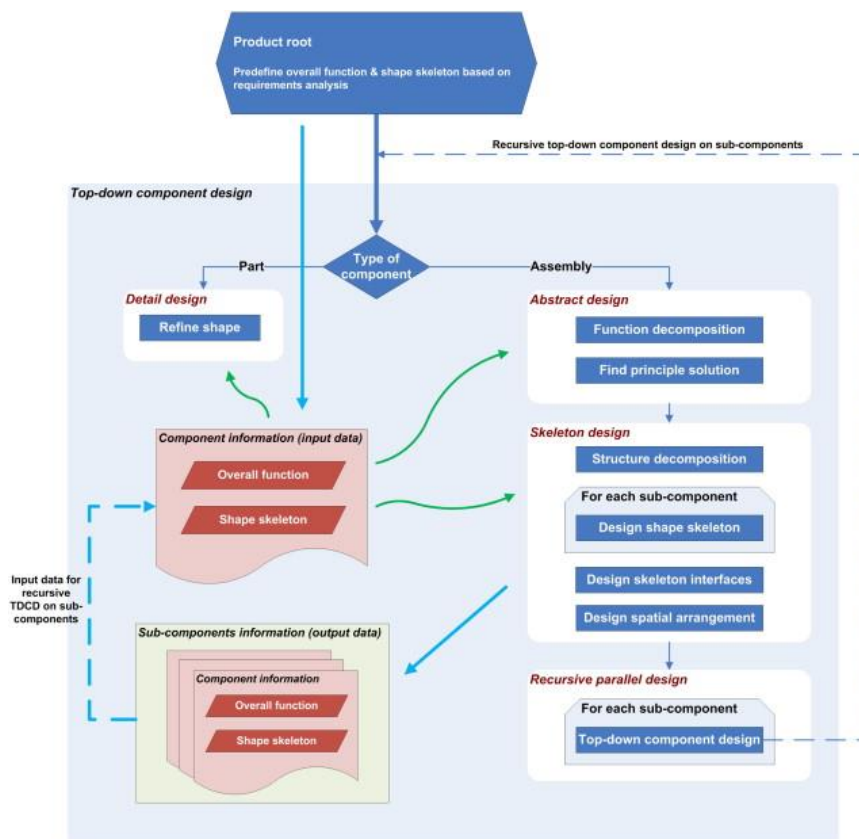
##### Optical properties

Transparency	①	Translucent
--------------	---	-------------

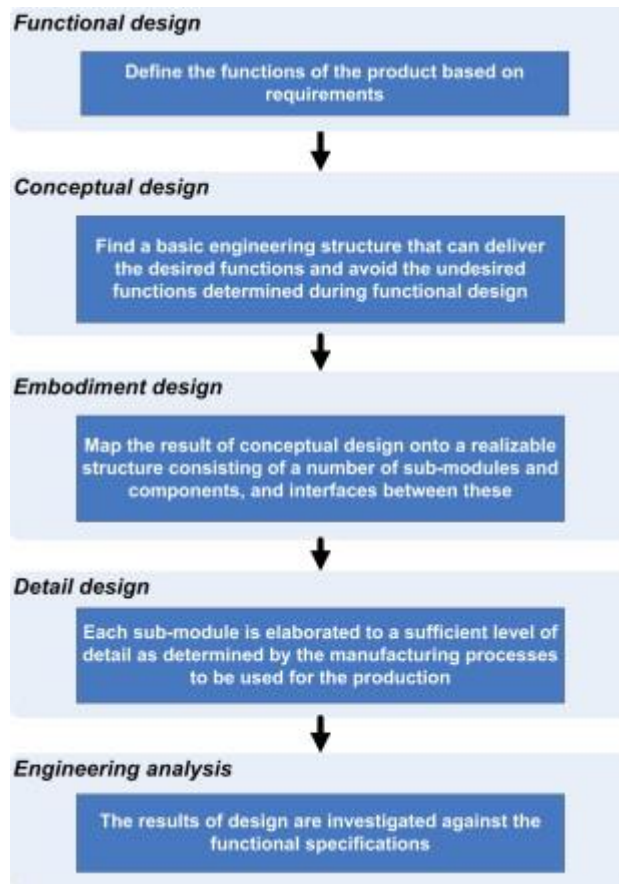
##### Processability

Castability	①	4	-	5
Moldability	①	4	-	5
Machinability	①	2	-	3
Weldability	①	1		


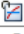


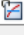
#### Item 5: Top Down Assembly Modelling Schematics<sup>[46]</sup>







## Item 6: Human Skin Properties (EduPack)<sup>[31]</sup>

Properties of Outline Row 4: Human Skin					
	A	B	C	D	E
1	Property	Value	Unit		
2	 Density	1200	kg m <sup>-3</sup>		
3	 Isotropic Elasticity				
4	Derive from	Young's Modulus and P...			
5	Young's Modulus	3E+06	Pa		
6	Poisson's Ratio	0.4			
7	Bulk Modulus	5E+06	Pa		
8	Shear Modulus	1.0714E+06	Pa		
9	 Tensile Yield Strength	1E+06	Pa		
10	 Compressive Yield Strength	1E+06	Pa		
11	 Tensile Ultimate Strength	8E+06	Pa		

### Item 7: Ansys Hand Calculations

Cushion area in contact with skin,  $A^* = 1225.712 \text{ mm}^2$   
 $= 0.001225712 \text{ m}^2$

\* = from inventor area inspection tool

$$F = 10 \text{ N}$$

$$\sigma = \frac{F}{A}$$























$$= \frac{10}{0.001225712}$$

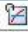





$$= 8158.523373 \text{ Pa}$$

$$= 0.008158523373 \text{ MPa}$$

This is an overestimate as the area is not incident to the direction of the force applied

### Item 8: Additional Cushion Materials For Ansys Simulation<sup>[31]</sup>

Properties of Outline Row 7: Silicone Elastomer					
	A	B	C	D	E
1	Property	Value	Unit		
2	 Density	1800	kg m <sup>-3</sup>		
3	 Isotropic Elasticity				
4	Derive from	Young's Modulus and...			
5	Young's Modulus	5E+06	Pa		
6	Poisson's Ratio	0.47			
7	Bulk Modulus	2.7778E+07	Pa		
8	Shear Modulus	1.7007E+06	Pa		
9	 Tensile Yield Strength	5.5E+06	Pa		
10	 Compressive Yield Strength	5.5E+06	Pa		
11	 Tensile Ultimate Strength	5.5E+06	Pa		
12	 Compressive Ultimate Strength	3E+07	Pa		

Properties of Outline Row 6: Natural Rubber					
	A	B	C	D	E
1	Property	Value	Unit		
2	 Density	930	kg m <sup>-3</sup>		
3	 Isotropic Elasticity				
4	Derive from	Young's Modulus and...			
5	Young's Modulus	2.5E+06	Pa		
6	Poisson's Ratio	0.49			
7	Bulk Modulus	4.1667E+07	Pa		
8	Shear Modulus	8.3893E+05	Pa		
9	 Tensile Yield Strength	3E+07	Pa		
10	 Compressive Yield Strength	3E+07	Pa		
11	 Tensile Ultimate Strength	3.2E+07	Pa		
12	 Compressive Ultimate Strength	3.3E+07	Pa		

### Item 9: Mask Cushion Production Economies Of Scale<sup>[42]</sup>

**Table II** RT related costs

<i>(I) Data acquisition and cushion design</i>	
(i) Material cost	NT\$25
Hydrogum (NT\$20)	
Plaster (NT\$5)	
(ii) Processing cost: CMM	NT\$80
(iii) Labor cost	NT\$180/h*1.5 h = NT\$270
Face model duplication (30 min)	
CMM operation (30 min)	
Data processing and cushion design (30 min)	
Total cost	NT\$375
<i>(II) RT fabrication</i>	
(i) Material cost: polymer	NT\$75
(ii) Processing cost: CNC	NT\$200
(iii) Labor cost	NT\$180/h*2 h = NT\$360
Tooling design (30 min)	
Process planning (30 min)	
Process handling (1 h)	
Total cost	NT\$635

**Table III** Costs of casting silicone per cushion

<i>(III) Casting silicone to create each cushion</i>	
(i) Material cost: silicone	NT\$30
(ii) Processing cost	NT\$80
Degassing (NT\$30)	
Oven (NT\$50)	
(iii) Labor cost: casting (20 min)	NT\$180/h*1/3 h = NT\$60
Total	NT\$170

**Table IV** Cost of multiple customized cushions and price-to-performance ratio

No. of cushion (n)	Unit cost ((I) + (II) + (III)*n)/n	Price (cost*2)	Performance (FF)	Price/performance
1	NT\$1,180	NT\$2,360	10	236
3	NT\$506.7	NT\$1,013.4	10	101.3
5	NT\$372	NT\$744	10	74.4
10	NT\$271	NT\$542	10	54.2
Commercial cushion		NT\$400	3.8	105.3